

Can Graph Neural Networks Count Substructures?

Zhengdao Chen^a, Lei Chen^a, Soledad Villar^{a, b}, and Joan Bruna^{a, b, c}

^aCourant Institute of Mathematical Sciences, New York University, New York

^bCenter for Data Science, New York University, New York

^cInstitute for Advanced Study, Princeton

Abstract

The ability to detect and count certain substructures in graphs is important for solving many tasks on graph-structured data, especially in the contexts of computational chemistry and biology as well as social network analysis. Inspired by this, we propose to study the expressive power of graph neural networks (GNNs) via their ability to count attributed graph substructures, extending recent works that examine their power in graph isomorphism testing and function approximation. We distinguish between two types of substructure counting: induced-subgraph-count and subgraph-count, and establish both positive and negative answers for popular GNN architectures. Specifically, we prove that Message Passing Neural Networks (MPNNs), 2-Weisfeiler-Lehman (2-WL) and 2-Invariant Graph Networks (2-IGNs) cannot perform induced-subgraph-count of substructures consisting of 3 or more nodes, while they can perform subgraph-count of star-shaped substructures. As an intermediary step, we prove that 2-WL and 2-IGNs are equivalent in distinguishing non-isomorphic graphs, partly answering an open problem raised in [Maron et al. \(2019a\)](#). We also prove positive results for k -WL and k -IGNs as well as negative results for k -WL with a finite number of iterations. We then conduct experiments that support the theoretical results for MPNNs and 2-IGNs. Moreover, motivated by substructure counting, we propose a local relational pooling approach with inspirations from [Murphy et al. \(2019\)](#) and demonstrate that it is not only effective for substructure counting but also able to achieve competitive performance on real-world tasks.

1 Introduction

In recent years, graph neural networks (GNNs) have achieved empirical success on processing data from various fields such as social networks, quantum chemistry, particle physics, knowledge graphs and combinatorial optimization ([Scarselli et al., 2008](#); [Bruna et al., 2013](#); [Duvenaud et al., 2015](#); [Kipf and Welling, 2016](#); [Defferrard et al., 2016](#); [Bronstein et al., 2017](#); [Dai et al., 2017](#); [Nowak et al., 2017](#); [Ying et al., 2018](#); [Zhou et al., 2018](#); [Choma et al., 2018](#); [Zhang and Chen, 2018](#); [You et al., 2018a,b, 2019a](#); [Yao et al., 2019](#); [Ding et al., 2019](#); [Sato et al., 2019](#); [Stokes et al., 2020](#)). Thanks to such progress, there have been growing interest in studying the expressive power of GNNs ([Sato, 2020](#)). One line of work does so by studying their ability to distinguish non-isomorphic graphs. In this regard, [Xu et al. \(2018a\)](#) and [Morris et al. \(2019\)](#) show that GNNs based on neighborhood-aggregation schemes are at most as powerful as the classical Weisfeiler-Lehman (WL) test ([Weisfeiler and Leman, 1968](#)) and propose GNN architectures that can achieve such level of power. While graph isomorphism testing is very interesting from a theoretical viewpoint, one may naturally wonder how relevant it is to real-world tasks on graph-structured data. Moreover, WL is powerful enough to distinguish almost all pairs of non-isomorphic graphs except for rare counterexamples ([Babai et al., 1980](#)). Hence, from the viewpoint of graph isomorphism testing, existing GNNs are in some sense already not far from being maximally powerful, which could make the pursuit of more powerful GNNs appear unnecessary.

Another perspective is the ability of GNNs to approximate permutation-invariant functions on graphs. For instance, [Maron et al. \(2019c\)](#) and [Keriven and Peyré \(2019\)](#) propose architectures that achieve universal approximation of permutation-invariant functions on graphs, though such models involve tensors with order growing in the size of the graph and are therefore impractical. [Chen et al. \(2019b\)](#) establishes an equivalence between the ability to distinguish any pair of non-isomorphic graphs and the ability to approximate arbitrary permutation-invariant functions on graphs. Nonetheless, for GNNs used in practice, which are not universally approximating, more efforts are needed to characterize what they can and cannot do. For example, [Loukas \(2019\)](#) shows that GNNs under assumptions are Turing universal but lose power when their depth and width are limited, though the arguments rely on the nodes all having distinct features and the focus is on the asymptotic depth-width tradeoff. Concurrently to our work, [Garg et al. \(2020\)](#) provide impossibility results of several classes of GNNs to decide graph properties including girth, circumference, diameter, radius, conjoint cycle, total number of cycles, and k -cliques. Despite these interesting results, we still need a perspective for understanding the expressive power of different classes of GNNs in a way that is intuitive, relevant to goals in practice, and potentially helpful in guiding the search for more powerful architectures.

In this work, we first establish a theoretical framework based on graph discrimination and function approximation for studying the ability of GNNs to count substructures in graphs with node and edge attributes. We distinguish between the counting of *subgraphs* and *induced subgraphs* that are isomorphic to a given pattern, and examine different GNN architectures. Our main contributions are:

- (1). We establish that neither Message Passing Neural Networks (MPNNs) ([Gilmer et al., 2017](#)) nor 2nd-order Invariant Graph Networks (2-IGNs) ([Maron et al., 2019c](#)) can count any connected *induced subgraph* of 3 or more nodes. For any such pattern, we prove this by constructing a pair of graphs that provably cannot be distinguished by any MPNN or 2-IGN but with different induced-subgraph-counts of the given pattern. This result points at an important class of simple-looking tasks that are provably hard for classical GNN architectures.
- (2). We show that MPNNs and 2-IGNs can count *subgraphs* that are star-shaped, thus generalizing the results in [Arvind et al. \(2018\)](#) to incorporate node and edge features. We also show that k -WL and k -IGNs can count *subgraphs* and *induced subgraphs* of size- k , which provides an intuitive understanding of the hierarchy of k -WL’s in terms of increasing power in counting substructures.
- (3). While a negative result for general k -WL is difficult to obtain, we show that running k -WL for at most T iterations is unable to count the number of *induced subgraphs* that are isomorphic to what we call path patterns of $(k + 1)2^T$ or more nodes. The result demonstrates an interplay between k and depth, an is relevant since real-life GNNs are often shallow.
- (4). To exploit the fact that substructures present themselves in local neighborhoods, we present a novel GNN architecture that we call *Local Relation Pooling*, with inspirations from [Murphy et al. \(2019\)](#). We empirically demonstrate that it performs both induced-subgraph-count and subgraph-count effectively on synthetic random graphs, while also achieving competitive performance on real molecular datasets.

2 Framework

2.1 Attributed graphs, graph isomorphism and (induced) subgraphs

We define an *attributed graph* as $G = (V, E, x, e)$, where $V = [n]$ is the set of vertices, $E \subset V \times V$ is the set of edges, $x_i \in \mathcal{X}$ represents the node feature (or node attribute) of node i , and $e_{i,j} \in \mathcal{Y}$ represent the edge feature of edge (i, j) if $(i, j) \in E$. For simplicity, we only consider undirected graphs and we

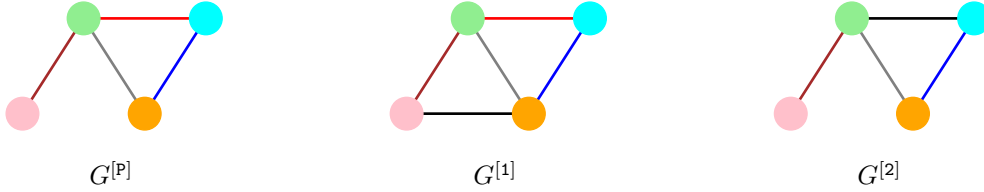


Figure 1: Illustration of the two types of counts of the pattern $G^{[P]}$ in graphs $G^{[1]}$ and $G^{[2]}$. The edge and node features are represented by colors. For $G^{[1]}$, the induced-subgraph-count $C_I(G^{[1]}; G^{[P]}) = 0$ but the subgraph-count $C_S(G^{[1]}; G^{[P]}) = 1$. For $G^{[2]}$, $C_I(G^{[2]}; G^{[P]}) = C_S(G^{[2]}; G^{[P]}) = 0$ since the edge features do not match.

do not allow self-connections or multi-edges. Note that an unattributed graph $G = (V, E)$ can be viewed as an attributed graph with identical node and edge features.

Unlike the node and edge features, the indices of the nodes are not inherent properties of the graph. Rather, different ways of ordering the nodes result in different representations of the same underlying graph. This is characterized by the definition of *graph isomorphism*: Two attributed graphs $G^{[1]} = (V^{[1]}, E^{[1]}, x^{[1]}, e^{[1]})$ and $G^{[2]} = (V^{[2]}, E^{[2]}, x^{[2]}, e^{[2]})$ are *isomorphic* if there exists a bijection $\pi : V^{[1]} \rightarrow V^{[2]}$ such that (1) $(i, j) \in E^{[1]}$ if and only if $(\pi(i), \pi(j)) \in E^{[2]}$, (2) $x_i^{[1]} = x_{\pi(i)}^{[2]}$ for all i in $V^{[1]}$, and (3) $e_{i,j}^{[1]} = e_{\pi(i),\pi(j)}^{[2]}$ for all $(i, j) \in E^{[1]}$.

For $G = (V, E, x, e)$, a *subgraph* of G can be represented by $G^{[S]} = (V^{[S]}, E^{[S]}, x, e)$ with $V^{[S]} \subseteq V$ and $E^{[S]} \subseteq E$. An *induced subgraph* of G can be represented by $G^{[S']} = (V^{[S']}, E^{[S']}, x, e)$ with $V^{[S']} \subseteq V$ and $E^{[S']} = E \cap (V^{[S']})^2$. In other words, the edge set of an induced subgraph needs to include all edges in E that have both end points belonging to $V^{[S']}$. Thus, an induced subgraph of G is also its subgraph, but the converse is not true.

2.2 Substructure counting

We now define two types of substructure counting associated with *subgraphs* and *induced subgraphs*, respectively, with an example illustrated in Figure 1. Let $G^{[P]} = (V^{[P]}, E^{[P]}, x^{[P]}, e^{[P]})$ be a (typically smaller) graph that we refer to as a *pattern* or *substructure*. We define $C_S(G, G^{[P]})$, called the *subgraph-count* of $G^{[P]}$ in G , to be the number of *subgraphs* of G that are isomorphic to $G^{[P]}$. We define $C_I(G, G^{[P]})$, called the *induced-subgraph-count* of $G^{[P]}$ in G , to be the number of *induced subgraphs* of G that are isomorphic to $G^{[P]}$. Since all induced subgraphs are subgraphs, we always have $C_I(G, G^{[P]}) \leq C_S(G, G^{[P]})$.

Below, we formally define the ability for certain function classes to count substructures as the ability to distinguish graphs with different subgraph or induced-subgraph counts of a given substructure.

Definition 1. Let \mathcal{G} be a space of graphs, and \mathcal{F} be a family of functions on \mathcal{G} . We say \mathcal{F} is able to perform *subgraph-count* (or *induced-subgraph-count*) of a pattern $G^{[P]}$ on \mathcal{G} if for all $G^{[1]}, G^{[2]} \in \mathcal{G}$ such that $C_S(G^{[1]}, G^{[P]}) \neq C_S(G^{[2]}, G^{[P]})$ (or $C_I(G^{[1]}, G^{[P]}) \neq C_I(G^{[2]}, G^{[P]})$), there exists $f \in \mathcal{F}$ that returns different outputs when applied to $G^{[1]}$ and $G^{[2]}$.

In Appendix A, we prove an equivalence between Definition 1 and the notion of approximating *subgraph-count* and *induced-subgraph-count* functions on the graph space. Definition 1 also naturally allows us to define the ability of graph isomorphism tests to count substructures: A graph isomorphism test, such as the Weisfeiler-Lehman (WL) test, takes as input a pair of graphs and returns

whether or not they are believed to be isomorphic. Typically, the test will return true if the two graphs are indeed isomorphic but does not necessarily return false for every pair of non-isomorphic graphs. Given such a graph isomorphism test, we say it is able to perform induced-subgraph-count (or subgraph-count) of a pattern $G^{[P]}$ on \mathcal{G} if $\forall G^{[1]}, G^{[2]} \in \mathcal{G}$ such that $C_I(G^{[1]}, G^{[P]}) \neq C_I(G^{[2]}, G^{[P]})$ (or $C_S(G^{[1]}, G^{[P]}) \neq C_S(G^{[2]}, G^{[P]})$), the test can distinguish these two graphs.

Additional notations that appear in the proofs are introduced in Appendix B. Next, we still study the ability of specific GNN models to count substructures.

3 MPNN and its higher-order generalizations

Message Passing Neural Network (MPNN) is a generic model that incorporates many popular architectures, and it is based on learning local aggregations of information in the graph (Gilmer et al., 2017). When applied to an undirected graph $G = (V, E, x, e)$, an MPNN with T layers is defined iteratively as follows. For $t < T$, to compute the message $m_i^{(t+1)}$ and the hidden state $h_i^{(t+1)}$ for each node $i \in V$ at the $(t + 1)$ th layer, we apply the following update rule:

$$m_i^{(t+1)} = \sum_{\mathcal{N}(i)} M_t(h_i^{(t)}, h_j^{(t)}, e_{i,j}), \quad h_i^{(t+1)} = U_t(h_i^{(t)}, m_i^{(t+1)})$$

where $\mathcal{N}(i)$ is the neighborhood of node i in G , M_t is the message function at layer t and U_t is the vertex update function at layer t . Finally, a graph-level prediction is computed as $\hat{y} = R(\{h_i^{(T)} : i \in V\})$, where R is the readout function. Typically, the hidden states at the first layer are set as $h_i^{(0)} = x_i$. Learnable parameters can appear in the functions M_t , U_t (for all $t \leq T$) and R .

Xu et al. (2018a) and Morris et al. (2019) show that, for graphs without edge features, such models are at most as powerful as the 1-Weisfeiler-Lehman (WL) test in distinguishing non-isomorphic graphs. Below, we will first extend this result to incorporate edge features, which MPNNs naturally accommodate. Then, this will allow us to understand the ability of MPNNs to count substructures by studying that of the WL tests.

3.1 The k -Weisfeiler-Lehman (k -WL) tests

For a positive integer k , the k -WL test is defined to take a pair of graphs $G^{[1]}$ and $G^{[2]}$ and outputs a judgment of whether they are isomorphic under the following procedure. For each of the graphs, the test assigns an initial ‘‘color’’ in some color space to every k -tuple in V^k according to its *isomorphism type*, and then updates its color iteratively according to the color of itself and its neighboring k -tuples in the previous iteration. The test will terminate and return the judgement that the two graphs are not isomorphic if at some iteration t , the multiset of the colors of all nodes differ for the two graphs. We refer the reader to Appendix C for a rigorous definition.

For each k , there exist pairs of non-isomorphic graphs that the k -WL test cannot determine as so. For $k \geq 2$, $(k + 1)$ -WL is strictly more powerful than k -WL, in the sense that there exist pairs of graphs distinguishable by the former but not the latter (Cai et al., 1992). Thus, with growing k , the set of k -WL tests forms a hierarchy with increasing discriminative power. For graphs *without* edges features, 1-WL and 2-WL are known to have the same discriminative power (Maron et al., 2019b). Note that there has been a different definition of WL in the literature, sometimes known as *Folklore Weisfeiler-Lehman* (FWL), and it is known that for $k \geq 2$, k -FWL has the same power as $(k + 1)$ -WL (Grohe and Otto, 2015; Maron et al., 2019b; Morris et al., 2019).¹

¹When the term ‘‘WL test’’ is used in the literature without a specific ‘‘ k ’’, it often refers to 1-WL, 2-WL or 1-FWL.

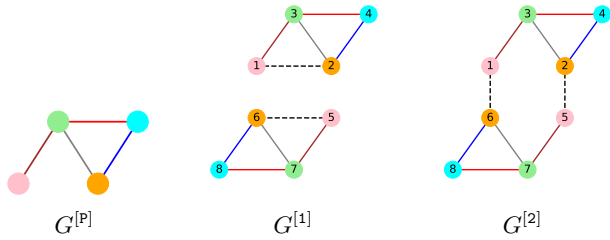


Figure 2: Illustration of the construction in the proof of Theorem 3 for the pattern $G^{[P]}$ on the left. Note that $C_I(G^{[1]}; G^{[P]}) = 0$ and $C_I(G^{[2]}; G^{[P]}) = 2$, while $G^{[1]}$ and $G^{[2]}$ cannot be distinguished by 2-WL, MPNNs or 2-IGNs.

As mentioned above, the following lemma extends Lemma 2 in Xu et al. (2018a) and Theorem 1 in Morris et al. (2019) to incorporate edge features. It is proved in Appendix D.

Lemma 2. *If two attributed graphs are indistinguishable by 2-WL, then they cannot be distinguished by any MPNN.*

Thus, this result motivates us to study what patterns 2-WL can and cannot count.

3.2 Substructure counting by 2-WL and MPNN

Whether or not 2-WL can perform induced-subgraph-count of a pattern is completely characterized by the number of nodes in the pattern. Any connected pattern with 1 or 2 nodes (i.e., representing a node or an edge) can be easily counted by an MPNN with 0 and 1 layer of message-passing, respectively, or by 2-WL with 0 iterations². In contrast, for all other patterns, we have the following negative result, which we prove in Appendix E.

Theorem 3. *2-WL cannot perform induced-subgraph-count of any connected pattern with 3 or more nodes.*

The intuition behind this result is that, given any connected pattern with 3 or more nodes, one can construct a pair of graphs (as illustrated in Figure 2) that have different induced-subgraph-counts of the pattern but cannot be distinguished by 2-WL. Thus, together with Theorem 2, we have

Corollary 4. *MPNNs cannot induced-subgraph-count any connected pattern with 3 or more nodes.*

For subgraph-count, if both nodes and edges are unweighted, Arvind et al. (2018) show that the only patterns 1-WL (and equivalently 2-WL) can count are either star-shaped patterns and pairs of disjoint edges. We prove the positive result that MPNNs can count star-shaped patterns even when node and edge features are allowed, owing to a result in Xu et al. (2018a) that the message functions are able to approximate any function on multisets.

Theorem 5. *MPNNs can perform subgraph-count of star-shaped patterns.*

By Theorem 2, this also implies that

Corollary 6. *2-WL can perform subgraph-count of star-shaped patterns.*

3.3 Substructure counting by generalizations of MPNN via k -WL

There have been efforts to extend the power of GNNs from the level of 1-WL to k -WL with larger k , such as Morris et al. (2019). Thus, it is also interesting to study what subgraphs k -WL can and cannot count. Since k -tuples are assigned initial colors based on their isomorphism types, the following is easily seen, and we provide a proof of it in Appendix G.

Theorem 7. *k -WL, at initialization, is able to perform both induced-subgraph-count and subgraph-count of patterns consisting of at most k nodes.*

²Rigorously, this is a special case of Theorem 7.

This establishes a potential hierarchy of increasing power in terms of substructure counting by k -WL. Nonetheless, negative results can be much harder to achieve. For example, to show that 2-FWL (and therefore 3-WL) cannot count cycles of length 8, [Fürier \(2017\)](#) has to rely on performing computer counting on the classical Cai-Fürier-Immerman counterexamples to k -WL ([Cai et al., 1992](#)). While we leave the pursuit of general and tighter characterizations of k -WL’s substructure counting power for future research, we provide a negative result concerning finite iterations of k -WL.

Definition 8. A path pattern of size m , denoted by H_m , is an unattributed graph, $H_m = (V^{[H_m]}, E^{[H_m]})$, where $V^{[H_m]} = [m]$, and $E^{[H_m]} = \{(i, i + 1) : 1 \leq i < m\} \cup \{(i + 1, i) : 1 \leq i < m\}$.

Theorem 9. Running T iterations of k -WL cannot perform induced-subgraph-count of any path pattern of $(k + 1)2^T$ or more nodes.

The proof with an illustration is given in [Appendix H](#). Though this bound grows quickly as T increases, in practice, many GNN models are designed to be shallow ([Zhou et al., 2018](#); [Wu et al., 2019](#)). Hence, this result is still relevant for studying finite-depth GNNs that are based on k -WL.

4 Invariant Graph Networks

Recently, diverging from the strategy of local aggregation of information as adopted by MPNNs and k -WLs, an alternative family of GNN models called *Invariant Graph Networks (IGNs)* was introduced in [Maron et al. \(2018, 2019c,b\)](#). Here we restate its definition.

Definition 10. A k th-order Invariant Graph Network (k -IGN) is a function $F : \mathbb{R}^{n^k \times d_0} \rightarrow \mathbb{R}$ that can be decomposed in the following way:

$$F = m \circ h \circ L^{(T)} \circ \sigma \circ \dots \circ \sigma \circ L^{(1)},$$

where each $L^{(t)}$ is a linear equivariant layer from $\mathbb{R}^{n^k \times d_{t-1}}$ to $\mathbb{R}^{n^k \times d_t}$, σ is a pointwise activation function, h is a linear invariant layer from $\mathbb{R}^{n^k \times d_T}$ to \mathbb{R} , and m is an MLP.

[Maron et al. \(2019c\)](#) show that if k is allowed to grow as a function of the size of the graphs, then k -IGNs can achieve universal approximation of permutation-invariant functions on graphs. In practice, due to the quick growth of computational complexity and implementation difficulty as k increases, having $k > 2$ is usually not practical. For $k = 2$, [Chen et al. \(2019b\)](#) proves that 2-IGNs are not universally approximating. However, it remains interesting to find more precise characterizations of the power of 2-IGNs.

In particular, 2-IGNs are known to be at least as powerful as 2-WL, by the other direction remains an open problem ([Maron et al., 2019c,a](#)). Here, we answer the question by proving the converse, that 2-IGNs are no more powerful than 2-WL. The proof can be found in [Appendix I](#).

Theorem 11. If two attributed graphs are indistinguishable by 2-WL, then no 2-IGN can distinguish them.

Corollary 12. 2-IGNs are exactly as powerful as 2-WL.

As a consequence of the equivalence stated above, the two following result follow [Theorem 3](#) and [Corollary 6](#) immediately. Note that we also provide a direct proof of [Corollary 13](#) in [Appendix J](#).

Corollary 13. 2-IGNs cannot perform induced-subgraph-count of any connected pattern with 3 or more nodes.

Corollary 14. 2-IGNs can perform subgraph-count of star-shaped patterns.

Moreover, since k -IGNs are no less powerful than k -WL ([Maron et al., 2019b](#)), we also have, as a corollary of [Theorem 7](#),

Corollary 15. k -IGNs can perform both induced-subgraph-count and subgraph-count of patterns consisting of at most k nodes.

5 Local Relational Pooling

Although MPNNs and 2-IGNs are able to aggregate information from multi-hop neighborhoods, our results show that the aggregation loses information such as the induced-subgraph-counts of nontrivial patterns. To bypass such limitations, we suggest going beyond the strategy of iteratively aggregating information in an inherently equivariant fashion, which underlies both MPNNs and IGNs.

We start with the observation that if a pattern is present in the graph, it can always be found in a sufficiently large local neighborhood, or *egonet*, of some node in the graph (Preciado et al., 2012). An egonet of depth l centered at a node i is defined as the induced subgraph consisting of i and all nodes within distance l from it. Note that any pattern with radius r is a subgraph of some egonet of depth $l = r$. Thus, by applying a powerful local model to each egonet separately and then aggregating the outputs, we can obtain a model capable of counting patterns. For such a local model, we adopt an approach of symmetrization by enumeration, similar to the Relational Pooling (RP) approach in Murphy et al. (2019) as well as the canonicalization mentioned in Duvenaud et al. (2015). In summary, it creates a powerful permutation-invariant model by symmetrizing a powerful model that is not necessarily permutation-invariant, where the symmetrization is performed by averaging or summing over all permutations of the nodes’ ordering. Formally, if $\mathbf{B} \in \mathbb{R}^{n \times n \times d}$ is a node-ordering-dependent representation of the graph G , we define

$$f_{\text{RP}}(G) = \sum_{\pi \in S_n} \bar{f}(\pi \circ \mathbf{B}),$$

where \bar{f} is a possibly non-permutation-invariant function, S_n is the set of permutations on n nodes, and $\pi \circ \mathbf{B}$ is \mathbf{B} transformed by permuting its first two dimensions according to π . Such f ’s are shown to be a universal approximators of permutation-invariant functions (Murphy et al., 2019). The summation quickly becomes intractable once n is large, and hence approximation methods have been introduced. In our case, however, since we apply this model to small egonets, the tractability issue is greatly alleviated. Moreover, since egonets are rooted graphs, we can reduce the symmetrization over all permutations in S_n to the subset $S_n^{\text{BFS}} \subseteq S_n$ of permutations compatible with breath-first-search (BFS) to further reduce the complexity, as suggested in Murphy et al. (2019).

Concretely, we define $G_{i,l}^{[\text{ego}]}$ as the egonet centered at node i of depth l , $n_{i,l}$ the number of nodes in $G_{i,l}^{[\text{ego}]}$, and $\mathbf{B}_{i,l}^{[\text{ego}]} \in \mathbb{R}^{n_i \times n_i \times d}$ the corresponding representation of $G_{i,l}^{[\text{ego}]}$. For computational efficiency, we crop $\mathbf{B}_{i,l}^{[\text{ego}]}$ into a fixed-sized subtensor for each egonet before applying RP. Thus, our model over the entire graph G is expressed as

$$f_{\text{LRP}}^{l,k}(G) = \sum_{i \in V} \sum_{\pi \in S_{n_{i,l}}^{\text{BFS}}} \bar{f}\left(C_k(\pi \circ \mathbf{B}_{i,l}^{[\text{ego}]})\right), \quad (1)$$

where we define $C_k(\mathbf{B}) = \mathbf{B}_{[k],[k],:} \in \mathbb{R}^{k \times k \times d}$. We call it depth- l size- k *Local Relational Pooling (LRP- l - k)*. If node degrees are upper-bounded by D , the time complexity is $O(n \cdot (D!)^{D^l} \cdot k^2)$, and hence linear in n if D, k and l are fixed. In the synthetic experiments below, we implement a variant of LRP-1-4 designed as, with the bias terms dropped,

$$\tilde{f}_{\text{LRP}}^{1,4}(G) = \mathbf{W}_1 \sum_{i \in V} \sigma \left[\frac{\text{MLP}(D_i)}{|S_{n_{i,1}}^{\text{BFS}}|} \odot \sum_{\pi \in S_{n_{i,1}}^{\text{BFS}}} f_*(\pi \circ \mathbf{B}_{i,1}^{[\text{ego}]}) \right], \quad (2)$$

where D_i is the degree of node i , σ is ReLU, MLP maps from \mathbb{R} to \mathbb{R}^H , where H is the hidden dimension, $\mathbf{W}_1 \in \mathbb{R}^{1 \times H}$ and $\forall j \in [H]$, $(f_*(\mathbf{X}))_j = \tanh(\sum \mathbf{W}_{2,j} \odot C_4(\mathbf{X})) \in \mathbb{R}$ with $\mathbf{W}_{2,j} \in \mathbb{R}^{4 \times 4 \times d}$. The motivation of $\text{MLP}(D_i)$ is to adaptively learn an invariant function over the permutations that is more general than summation or averaging.

A drawback of the LRP model introduced above is that it is unable to exploit non-local information beyond the depth- l egonet. Hence, we take a step further and propose to apply LRP iteratively to gather multi-hop information. Practically, we pre-compute and store a mapping $\mathcal{I} : \mathbf{B} \mapsto C_k(\pi \circ \mathbf{B}^{\text{[ego]}})$ so that it can be called iteratively. Moreover, operations in \mathcal{I} can take advantage of sparse matrix multiplication as well as graph batching, further enhancing the efficiency. We refer to this new model as *Deep Local Relational Pooling (Deep LRP)*, and describe it in more details in Appendix K. We perform experiments on both synthetic tasks and molecular prediction tasks with Deep LRP.

6 Numerical experiments

6.1 Synthetic tasks

We verify our theoretical results on the five graph-level regression tasks illustrated in Figure 3. By Theorem 3 and Corollary 4, MPNNs and 2-IGNs cannot perform induced-subgraph-count of any patterns with 3 or more nodes. Note that since a triangle is a clique, its induced-subgraph-count and subgraph-count are equal. We generate the ground-truth counts of these unattributed and attributed patterns in each graph with an counting algorithm proposed by Shervashidze et al. (2009). By Theorem 5 and Corollary 6, MPNNs and 2-IGNs can perform subgraph-count but not induced-subgraph-count of 3-stars.

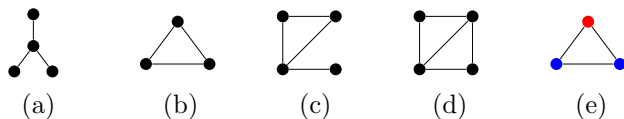


Figure 3: Substructures to be counted in the experiments: (a) 3-star (b) triangle (c) tailed triangle (d) chordal cycle (e) attributed triangle.

Datasets. We generate two synthetic datasets of random unattributed graphs. The first one is a set of 5000 Erdős-Renyi random graphs denoted as $ER(m, p)$, where $m = 10$ is the number of nodes in each graph and $p = 0.3$ is the probability that an edge exists. The second one is a set of 5000 random regular graphs (Steger and Wormald, 1999) denoted as $RG(m, d)$, where m is the number of nodes in each graph and d is the node degree. We uniformly sample (m, d) from $\{(10, 6), (15, 6), (20, 5), (30, 5)\}$. We also randomly delete m edges in each graph from the second dataset. For both datasets, we randomly split them into training-validation-test sets with percentages 30%-20%-50%. For the attributed task, we mark nodes with even indices as red and nodes with odd indices as blue, and set the color as node feature.

Models. We consider LRP, GIN (Xu et al., 2018a), GCN (Kipf and Welling, 2016), 2-IGN (Maron et al., 2018), PPGN (Maron et al., 2019b) and spectral GNN (sGNN) (Chen et al., 2019a), with GIN and GCN belonging to the category of MPNNs. Details of GNN architectures are provided in Appendix L. We use mean squared error (MSE) for regression loss. Each model is trained on 1080ti five times with different random seeds.

Results. The results on the two tasks of unattributed triangles and 3-stars are shown in Table 1, measured by the MSE on the test set divided by the variance of the ground truth counts of the pattern computed over all graphs in the dataset. Results on all the other synthetic tasks are shown in Appendix M. Firstly, the almost-negligible errors of LRP on all the tasks supports our theory that depth-1 LRP is powerful enough for counting triangles and 3-stars, both of which are patterns with radius 1. GIN, 2-IGN and sGNN produce much smaller test error than the variance of the ground truth counts for the 3-star tasks, consistent with their theoretical power to perform subgraph-count of stars. Relative to the variance of the ground truth counts, GIN and 2-IGN have worse top performance on the triangle task than on the 3-star task, also as expected from the theory. PPGN (Maron et al., 2019b) with 3-WL discrimination power also works well on both counting triangles and 3-stars. Moreover, the experiment results provide interesting insights into the average-case performance in

the substructure counting tasks, which are beyond what our theory is able to predict.

Table 1: Performance of different GNNs on learning the induced-subgraph-count of triangles and the subgraph-count of 3-stars on the two datasets, measured by test MSE divided by variance of the ground truth counts. Shown here are the best and the median performances of each model over five runs. We select the best out of four variants for each of GCN, GIN and sGNN, and the better out of two variants for 2-IGN. Details of the GNN architectures and results on other synthetic tasks can be found in Appendices L, M.

	Erdős-Renyi				Random Regular			
	Triangle		3-Star		Triangle		3-Star	
	top 1	top 3	top 1	top 3	top 1	top 3	top 1	top 3
LRP-1-4	1.56E-4	2.49E-4	2.17E-5	5.23E-5	2.47E-4	3.83E-4	1.88E-6	2.81E-6
Deep LRP-1-4	2.81E-5	4.77E-5	1.12E-5	3.78E-5	1.30E-6	5.16E-6	2.07E-6	4.97E-6
2-IGN	9.83E-2	9.85E-1	5.40E-4	5.12E-2	2.62E-1	5.96E-1	1.19E-2	3.28E-1
PPGN	5.08E-8	2.51E-7	4.00E-5	6.01E-5	1.40E-6	3.71E-5	8.49E-5	9.50E-5
GIN	1.23E-1	1.25E-1	1.62E-4	3.44E-4	4.70E-1	4.74E-1	3.73E-4	4.65E-4
GCN	6.78E-1	8.27E-1	4.36E-1	4.55E-1	1.82	2.05	2.63	2.80
sGNN	9.25E-2	1.13E-1	2.36E-3	7.73E-3	3.92E-1	4.43E-1	2.37E-2	1.41E-1

6.2 Real-world tasks

We evaluate Deep LRP on the molecular datasets `ogbg-molhiv` (Wu et al., 2018) and `QM9` (Ramakrishnan et al., 2014), which consist of molecular graphs with bounded degrees and are therefore suitable for the permutation computations in LRP. More details of the experimental setup can be found in Appendix N.

Results. The results on the `ogbg-molhiv` and `QM9` are shown in Tables 2 and 3. On `ogbg-molhiv`, Deep LRP-1-4 outperforms all baselines without the virtual node. To avoid overfitting, we also train Deep LRP-1-4 with fewer epochs and achieve better test performance. On `QM9`, Deep LRP-1-4 largely outperforms MPNN and achieves comparable performance with baselines that are more powerful than 1-WL including 123-gnn and PPGN.

7 Conclusions

In this work, we establish a theoretical framework for studying the expressive power of classes of GNNs based on their ability to count substructures. We distinguish between two kinds of counting: subgraph-count and induced-subgraph-count, and prove an equivalence between approximating the (induced)-subgraph-count functions and discriminating graphs with different (induced)-subgraph-counts of a given pattern. Then, examining specific GNN architectures, we prove that neither MPNNs nor 2-IGNs can perform induced-subgraph-count of any connected structure with 3 or more nodes; k -IGNs and k -WL can perform subgraph-count and induced-subgraph-count of any pattern of size k . We also provide an upper bound on the size of the “path-shaped” substructures whose induced-subgraph-count can be performed by finite iterations of k -WL. Also, as intermediary results, we prove that MPNNs are no more powerful than 2-WL on edge-attributed graphs, and that 2-IGNs are equivalent to 2-WL in distinguishing non-isomorphic graphs, which partly answers an open problem raised in Maron et al. (2019a). In addition, we perform numerical experiments that support our theoretical results and show that our Local Relational Pooling approach can successfully count certain substructures as well as achieve competitive performance on real molecular datasets. In summary, we build a theoretical foundation for using substructure counting as an intuitive and relevant measure of the expressive power of GNNs, and our concrete results for existing GNNs

Table 2: Performance of different GNNs on a molecule dataset **ogbg-molhiv**, measured by test ROC-AUC (%) for molecule property binary classification. We report the mean and standard deviation of all training and test results corresponding to the best validation results. Details of LRP-1-4 and LRP-1-4 (ES) can be found in Appendices L, N. ES stands for early stopping (20 epochs of training). LRP-1-4 is trained with 10 runs and LRP-1-4 (ES) is trained with 35 runs. †: reported on the OGB leaderboard (Hu et al., 2020). ‡: reported by Hu et al. (2019).

Model	Training	Validation	Testing
Deep LRP-1-4	89.81±2.90	81.31±0.88	76.87±1.80
Deep LRP-1-4 (ES)	87.56±2.11	82.09±1.16	77.19±1.40
GIN†	88.64±2.54	82.32±0.90	75.58±1.40
GIN + VN†	92.73±3.80	84.79±0.68	77.07±1.49
GCN†	88.54±2.19	82.04±1.41	76.06±0.97
GCN + VN†	90.07±4.69	83.84±0.91	75.99±1.19
GAT ‡	-	-	72.9±1.8
GraphSAGE ‡	-	-	74.4±0.7

Table 3: Performance of different GNNs on a molecule dataset **QM9**, measured by test Mean Absolute Error for molecule property regression. All baselines are taken from (Maron et al., 2019b), including DTNN (Wu et al., 2018) and 123-gnn (Morris et al., 2019).

Target	DTNN	MPNN	123-gnn	PPGN	Deep LRP-1-4
μ	0.244	0.358	0.476	0.231	0.390
α	0.95	0.89	0.27	0.382	0.312
ϵ_{homo}	0.00388	0.00541	0.00337	0.00276	0.00279
ϵ_{lumo}	0.00512	0.00623	0.00351	0.00287	0.00295
$\Delta\epsilon$	0.0112	0.0066	0.0048	0.00406	0.00388
$\langle R^2 \rangle$	17	28.5	22.9	16.07	19.4
ZPVE	0.00172	0.00216	0.00019	0.00064	0.00059
U_0	2.43	2.05	0.0427	0.234	0.499
U	2.43	2	0.111	0.234	0.499
H	2.43	2.02	0.0419	0.229	0.498
G	2.43	2.02	0.0469	0.238	0.498
C_v	0.27	0.42	0.0944	0.184	0.135
Loss	0.1014	0.1108	0.0657	0.0512	0.0611

motivate the search for more powerful designs of GNNs.

One limitation of our theory is that it only pertains to the expressive power of GNNs and does not speak about optimization or generalization. In addition, our theoretical results are worse-case in nature and cannot predict average-case performance. Many interesting questions remain, including better characterizing the substructure-counting ability of general k -WL and k -IGNs as well as other architectures such as spectral GNNs (Chen et al., 2019a), polynomial IGNs (Maron et al., 2019a) and P-GNNs (You et al., 2019b), to name a few. Another interesting future direction is to study the relevance of substructure counting in empirical tasks, following the work of Ying et al. (2019). Finally, we hope our framework can help guide the search for more powerful GNNs by having substructure counting as a criterion.

Acknowledgements

We would like to thank Haggai Maron, Jiaxuan You, Ryoma Sato and Christopher Morris for helpful conversations. This work is partially supported by the Alfred P. Sloan Foundation, NSF RI-1816753, NSF CAREER CIF 1845360, NSF CHS-1901091, Samsung Electronics, and the Institute for Advanced Study. SV is partly supported by NSF DMS 1913134, EOARD FA9550-18-1-7007 and the Simons Algorithms and Geometry (A&G) Think Tank.

Broader impact

In this work we propose to understand the power of GNN architectures via the substructures that they can and cannot count. Our work is motivated by the relevance of detecting and counting *graph substructures* in applications, and the current trend on using deep learning, and in particular graph neural networks in such scientific fields.

Also referred to by various names including *graphlets*, *motifs*, *subgraphs* and *graph fragments*, graph substructures are well-studied and relevant for graph-related tasks in computational chemistry (Deshpande et al., 2002; Murray and Rees, 2009; Duvenaud et al., 2015; Jin et al., 2018, 2019,

2020), computational biology (Koyutrk et al., 2004) and social network studies (Jiang et al., 2010). In organic chemistry, for example, certain patterns of atoms called functional groups are usually considered indicative of the molecules’ properties (Lemke, 2003; Pope et al., 2018). In the literature of molecular chemistry, substructure counts have been used to generate molecular fingerprints (Morgan, 1965; OBoyle and Sayle, 2016) and compute similarities between molecules (Alon et al., 2008; Rahman et al., 2009). In addition, for general graphs, substructure counts have been used to create graph kernels (Shervashidze et al., 2009) and compute spectral information (Preciado and Jadbabaie, 2010). The connection between GNNs and graph substructures is explored empirically by Ying et al. (2019) to interpret the predictions made by GNNs.

Thus, the ability of different GNN architectures to count graph substructures not only serves as an intuitive theoretical measure of their expressive power but also is highly relevant to real-world scenarios. While people have proposed variants of GNNs that take advantage of substructure information (Monti et al., 2018; Liu et al., 2018, 2019; Bouritsas et al., 2020), often they rely on handcrafting rather than learning such information. Our results not only proposes a GNN that has the ability to count certain substructures, but also it shows that some widely used GNN architectures are not able to count substructures nor distinguish graphs with different substructure counts. Such knowledge may indicate that some widely-used graph neural network architectures are actually not the right tool for certain scientific problems.

References

- Alon, N., Dao, P., Hajirasouliha, I., Hormozdiari, F., and Sahinalp, S. C. (2008). Biomolecular network motif counting and discovery by color coding. *Bioinformatics*, 24(13):i241–i249.
- Arvind, V., Fuhlbrück, F., Köbler, J., and Verbitsky, O. (2018). On weisfeiler-leman invariance: Subgraph counts and related graph properties. *arXiv preprint arXiv:1811.04801*.
- Babai, L., Erdos, P., and Selkow, S. M. (1980). Random graph isomorphism. *SIAM Journal on computing*, 9(3):628–635.
- Bouritsas, G., Frasca, F., Zafeiriou, S., and Bronstein, M. M. (2020). Improving graph neural network expressivity via subgraph isomorphism counting. *arXiv preprint arXiv:2006.09252*.
- Bronstein, M. M., Bruna, J., LeCun, Y., Szlam, A., and Vandergheynst, P. (2017). Geometric deep learning: Going beyond euclidean data. *IEEE Signal Processing Magazine*, 34(4):18–42.
- Bruna, J., Zaremba, W., Szlam, A., and LeCun, Y. (2013). Spectral networks and locally connected networks on graphs. *arXiv preprint arXiv:1312.6203*.
- Cai, J.-Y., Fürer, M., and Immerman, N. (1992). An optimal lower bound on the number of variables for graph identification. *Combinatorica*, 12(4):389–410.
- Chen, Z., Li, L., and Bruna, J. (2019a). Supervised community detection with line graph neural networks. *International Conference on Learning Representations*.
- Chen, Z., Villar, S., Chen, L., and Bruna, J. (2019b). On the equivalence between graph isomorphism testing and function approximation with gnn. In *Advances in Neural Information Processing Systems*, pages 15868–15876.
- Choma, N., Monti, F., Gerhardt, L., Palczewski, T., Ronaghi, Z., Prabhat, P., Bhimji, W., Bronstein, M., Klein, S., and Bruna, J. (2018). Graph neural networks for icecube signal classification. In *2018 17th IEEE International Conference on Machine Learning and Applications (ICMLA)*, pages 386–391. IEEE.

- Cybenko, G. (1989). Approximation by superpositions of a sigmoidal function. *Mathematics of control, signals and systems*, 2(4):303–314.
- Dai, H., Khalil, E. B., Zhang, Y., Dilkina, B., and Song, L. (2017). Learning combinatorial optimization algorithms over graphs. *arXiv preprint arXiv: 1704.01665*.
- Defferrard, M., Bresson, X., and Vandergheynst, P. (2016). Convolutional neural networks on graphs with fast localized spectral filtering. In *Advances in neural information processing systems*, pages 3844–3852.
- Deshpande, M., Kuramochi, M., and Karypis, G. (2002). Automated approaches for classifying structures. Technical report, Minnesota University Minneapolis Department of Computer Science.
- Ding, M., Zhou, C., Chen, Q., Yang, H., and Tang, J. (2019). Cognitive graph for multi-hop reading comprehension at scale. In *Proceedings of the 57th Annual Meeting of the Association for Computational Linguistics*, pages 2694–2703, Florence, Italy. Association for Computational Linguistics.
- Duvenaud, D. K., Maclaurin, D., Iparraguirre, J., Bombarell, R., Hirzel, T., Aspuru-Guzik, A., and Adams, R. P. (2015). Convolutional networks on graphs for learning molecular fingerprints. In *Advances in neural information processing systems*, pages 2224–2232.
- Fey, M. and Lenssen, J. E. (2019). Fast graph representation learning with pytorch geometric.
- Fürer, M. (2017). On the combinatorial power of the Weisfeiler-Lehman algorithm. *arXiv preprint arXiv:1704.01023*.
- Garg, V. K., Jegelka, S., and Jaakkola, T. (2020). Generalization and representational limits of graph neural networks.
- Gilmer, J., Schoenholz, S. S., Riley, P. F., Vinyals, O., and Dahl, G. E. (2017). Neural message passing for quantum chemistry. In *Proceedings of the 34th International Conference on Machine Learning-Volume 70*, pages 1263–1272. JMLR. org.
- Grohe, M. and Otto, M. (2015). Pebble games and linear equations. *The Journal of Symbolic Logic*, pages 797–844.
- He, K., Zhang, X., Ren, S., and Sun, J. (2015). Deep residual learning for image recognition.
- Hornik, K. (1991). Approximation capabilities of multilayer feedforward networks. *Neural Networks*, 4:251–257.
- Hu, W., Fey, M., Zitnik, M., Dong, Y., Ren, H., Liu, B., Catasta, M., and Leskovec, J. (2020). Open graph benchmark: Datasets for machine learning on graphs. *arXiv preprint arXiv:2005.00687*.
- Hu, W., Liu, B., Gomes, J., Zitnik, M., Liang, P., Pande, V., and Leskovec, J. (2019). Strategies for pre-training graph neural networks. In *International Conference on Learning Representations*.
- Ioffe, S. and Szegedy, C. (2015). Batch normalization: Accelerating deep network training by reducing internal covariate shift. *arXiv preprint arXiv:1502.03167*.
- Jiang, C., Coenen, F., and Zito, M. (2010). Finding frequent subgraphs in longitudinal social network data using a weighted graph mining approach. In *International Conference on Advanced Data Mining and Applications*, pages 405–416. Springer.
- Jin, W., Barzilay, R., and Jaakkola, T. (2019). Hierarchical graph-to-graph translation for molecules.

- Jin, W., Barzilay, R., and Jaakkola, T. (2020). Composing molecules with multiple property constraints. *arXiv preprint arXiv:2002.03244*.
- Jin, W., Barzilay, R., and Jaakkola, T. S. (2018). Junction tree variational autoencoder for molecular graph generation. *CoRR*, abs/1802.04364.
- Keriven, N. and Peyré, G. (2019). Universal invariant and equivariant graph neural networks. *arXiv preprint arXiv:1905.04943*.
- Kingma, D. P. and Ba, J. (2014). Adam: A method for stochastic optimization. *arXiv preprint arXiv:1412.6980*.
- Kipf, T. N. and Welling, M. (2016). Semi-supervised classification with graph convolutional networks. *arXiv preprint arXiv:1609.02907*.
- Koyutrk, M., Grama, A., and Szpankowski, W. (2004). An efficient algorithm for detecting frequent subgraphs in biological networks. *Bioinformatics*, 20(suppl 1):i200–i207.
- Lemke, T. L. (2003). *Review of organic functional groups: introduction to medicinal organic chemistry*. Lippincott Williams & Wilkins.
- Liu, S., Chandereng, T., and Liang, Y. (2018). N-gram graph, A novel molecule representation. *arXiv preprint arXiv:1806.09206*.
- Liu, X., Pan, H., He, M., Song, Y., and Jiang, X. (2019). Neural subgraph isomorphism counting.
- Loukas, A. (2019). What graph neural networks cannot learn: depth vs width. *arXiv preprint arXiv:1907.03199*.
- Maron, H., Ben-Hamu, H., and Lipman, Y. (2019a). Open problems: Approximation power of invariant graph networks.
- Maron, H., Ben-Hamu, H., Serviansky, H., and Lipman, Y. (2019b). Provably powerful graph networks. In *Advances in Neural Information Processing Systems*, pages 2153–2164.
- Maron, H., Ben-Hamu, H., Shamir, N., and Lipman, Y. (2018). Invariant and equivariant graph networks.
- Maron, H., Fetaya, E., Segol, N., and Lipman, Y. (2019c). On the universality of invariant networks. *arXiv preprint arXiv:1901.09342*.
- Monti, F., Otness, K., and Bronstein, M. M. (2018). Motifnet: a motif-based graph convolutional network for directed graphs. *CoRR*, abs/1802.01572.
- Morgan, H. L. (1965). The generation of a unique machine description for chemical structures—a technique developed at chemical abstracts service. *Journal of Chemical Documentation*, 5(2):107–113.
- Morris, C., Ritzert, M., Fey, M., Hamilton, W. L., Lenssen, J. E., Rattan, G., and Grohe, M. (2019). Weisfeiler and leman go neural: Higher-order graph neural networks. *Association for the Advancement of Artificial Intelligence*.
- Murphy, R. L., Srinivasan, B., Rao, V., and Ribeiro, B. (2019). Relational pooling for graph representations. *arXiv preprint arXiv:1903.02541*.
- Murray, C. W. and Rees, D. C. (2009). The rise of fragment-based drug discovery. *Nature chemistry*, 1(3):187.

- Nowak, A., Villar, S., Bandeira, A. S., and Bruna, J. (2017). A note on learning algorithms for quadratic assignment with graph neural networks. *arXiv preprint arXiv:1706.07450*.
- OBoyle, N. M. and Sayle, R. A. (2016). Comparing structural fingerprints using a literature-based similarity benchmark. *Journal of cheminformatics*, 8(1):1–14.
- Pope, P., Kolouri, S., Rostrami, M., Martin, C., and Hoffmann, H. (2018). Discovering molecular functional groups using graph convolutional neural networks. *arXiv preprint arXiv:1812.00265*.
- Preciado, V. M., Draief, M., and Jadbabaie, A. (2012). Structural analysis of viral spreading processes in social and communication networks using egonets.
- Preciado, V. M. and Jadbabaie, A. (2010). From local measurements to network spectral properties: Beyond degree distributions. In *49th IEEE Conference on Decision and Control (CDC)*, pages 2686–2691. IEEE.
- Rahman, S. A., Bashton, M., Holliday, G. L., Schrader, R., and Thornton, J. M. (2009). Small molecule subgraph detector (smsd) toolkit. *Journal of cheminformatics*, 1(1):12.
- Ramakrishnan, R., Dral, P. O., Rupp, M., and Von Lilienfeld, O. A. (2014). Quantum chemistry structures and properties of 134 kilo molecules. *Scientific data*, 1:140022.
- Sato, R. (2020). A survey on the expressive power of graph neural networks. *arXiv preprint arXiv:2003.04078*.
- Sato, R., Yamada, M., and Kashima, H. (2019). Approximation ratios of graph neural networks for combinatorial problems. In Wallach, H., Larochelle, H., Beygelzimer, A., d'Alché-Buc, F., Fox, E., and Garnett, R., editors, *Advances in Neural Information Processing Systems 32*, pages 4081–4090. Curran Associates, Inc.
- Scarselli, F., Gori, M., Tsoi, A. C., Hagenbuchner, M., and Monfardini, G. (2008). The graph neural network model. *IEEE Transactions on Neural Networks*, 20(1):61–80.
- Shervashidze, N., Vishwanathan, S., Petri, T., Mehlhorn, K., and Borgwardt, K. (2009). Efficient graphlet kernels for large graph comparison. In *Artificial Intelligence and Statistics*, pages 488–495.
- Steger, A. and Wormald, N. C. (1999). Generating random regular graphs quickly. *Combinatorics, Probability and Computing*, 8(4):377–396.
- Stokes, J. M., Yang, K., Swanson, K., Jin, W., Cubillos-Ruiz, A., Donghia, N. M., MacNair, C. R., French, S., Carfrae, L. A., Bloom-Ackerman, Z., et al. (2020). A deep learning approach to antibiotic discovery. *Cell*, 180(4):688–702.
- Ulyanov, D., Vedaldi, A., and Lempitsky, V. (2016). Instance normalization: The missing ingredient for fast stylization. *arXiv preprint arXiv:1607.08022*.
- Wang, M., Yu, L., Zheng, D., Gan, Q., Gai, Y., Ye, Z., Li, M., Zhou, J., Huang, Q., Ma, C., Huang, Z., Guo, Q., Zhang, H., Lin, H., Zhao, J., Li, J., Smola, A., and Zhang, Z. (2019). Deep graph library: Towards efficient and scalable deep learning on graphs.
- Weisfeiler, B. and Leman, A. (1968). The reduction of a graph to canonical form and the algebra which appears therein. *Nauchno-Technicheskaya Informatsia*, 2(9):12-16.
- Wu, Z., Pan, S., Chen, F., Long, G., Zhang, C., and Yu, P. S. (2019). A comprehensive survey on graph neural networks. *arXiv preprint arXiv:1901.00596*.

- Wu, Z., Ramsundar, B., Feinberg, E. N., Gomes, J., Geniesse, C., Pappu, A. S., Leswing, K., and Pande, V. (2018). Moleculenet: a benchmark for molecular machine learning. *Chemical science*, 9(2):513–530.
- Xu, K., Hu, W., Leskovec, J., and Jegelka, S. (2018a). How powerful are graph neural networks? *arXiv preprint arXiv:1810.00826*.
- Xu, K., Li, C., Tian, Y., Sonobe, T., Kawarabayashi, K.-i., and Jegelka, S. (2018b). Representation learning on graphs with jumping knowledge networks. *arXiv preprint arXiv:1806.03536*.
- Yao, W., Bandeira, A. S., and Villar, S. (2019). Experimental performance of graph neural networks on random instances of max-cut. In *Wavelets and Sparsity XVIII*, volume 11138, page 111380S. International Society for Optics and Photonics.
- Ying, R., Bourgeois, D., You, J., Zitnik, M., and Leskovec, J. (2019). Gnn explainer: A tool for post-hoc explanation of graph neural networks. *arXiv preprint arXiv:1903.03894*.
- Ying, R., You, J., Morris, C., Ren, X., Hamilton, W. L., and Leskovec, J. (2018). Hierarchical graph representation learning with differentiable pooling. *CoRR*, abs/1806.08804.
- You, J., Liu, B., Ying, Z., Pande, V., and Leskovec, J. (2018a). Graph convolutional policy network for goal-directed molecular graph generation. In *Advances in neural information processing systems*, pages 6410–6421.
- You, J., Wu, H., Barrett, C., Ramanujan, R., and Leskovec, J. (2019a). G2sat: Learning to generate sat formulas. In Wallach, H., Larochelle, H., Beygelzimer, A., d'Alché-Buc, F., Fox, E., and Garnett, R., editors, *Advances in Neural Information Processing Systems 32*, pages 10553–10564. Curran Associates, Inc.
- You, J., Ying, R., and Leskovec, J. (2019b). Position-aware graph neural networks. *arXiv preprint arXiv:1906.04817*.
- You, J., Ying, R., Ren, X., Hamilton, W. L., and Leskovec, J. (2018b). Graphrnn: A deep generative model for graphs. *CoRR*, abs/1802.08773.
- Zaheer, M., Kottur, S., Ravanbakhsh, S., Póczos, B., Salakhutdinov, R. R., and Smola, A. J. (2017). Deep sets. In *Advances in neural information processing systems*, pages 3391–3401.
- Zhang, M. and Chen, Y. (2018). Link prediction based on graph neural networks. In *Advances in Neural Information Processing Systems*, pages 5165–5175.
- Zhou, J., Cui, G., Zhang, Z., Yang, C., Liu, Z., Wang, L., Li, C., and Sun, M. (2018). Graph neural networks: A review of methods and applications. *arXiv preprint arXiv:1812.08434*.

A Function approximation perspective of substructure counting

On a space of graphs \mathcal{G} , we call $C_I(\cdot; G^{[P]})$ the *induced-subgraph-count function* of the pattern $G^{[P]}$, and $C_S(\cdot; G^{[P]})$ the *subgraph-count function* of $G^{[P]}$. To formalize the probe into whether certain GNN architectures can count different substructures, a natural question to study is whether they are able to approximate the induced-subgraph-count and the subgraph-count functions arbitrarily well. Formally, given a target function $g : \mathcal{G} \rightarrow \mathbb{R}$, and family of functions, \mathcal{F} , which in our case is typically the family of functions that a GNN architecture can represent, we say \mathcal{F} is able to approximate g on \mathcal{G} if for all $\epsilon > 0$ there exists $f \in \mathcal{F}$ such that $|g(G) - f(G)| < \epsilon$, for all $G \in \mathcal{G}$.

Nonetheless, such criterion based on function approximation is hard to work with directly when we look at concrete examples later on. For this reason, in the main text we work with an alternative definition, Definition 1, based on distinguishing graphs with different substructure counts. Below, we show the equivalence between these two perspectives.

A.1 From function approximation to graph discrimination

Say \mathcal{G} is a space of graphs, and \mathcal{F} is a family of functions from \mathcal{G} to \mathbb{R} . Given two graphs $G^{[1]}, G^{[2]} \in \mathcal{G}$, we say \mathcal{F} is able to distinguish them if there exists $f \in \mathcal{F}$ such that $f(G^{[1]}) \neq f(G^{[2]})$. Such a perspective has been explored in Chen et al. (2019b), for instance, to build an equivalence between function approximation and graph isomorphism testing by GNNs. In the context of substructure counting, it is clear that the ability to approximate the count functions entails the ability to distinguish graphs in the following sense:

Observation 1. *If \mathcal{F} is able to approximate the induced-subgraph-count (or subgraph-count) function of a pattern $G^{[P]}$ on the space \mathcal{G} , then for all $G^{[1]}, G^{[2]} \in \mathcal{G}$ such that $C_I(G^{[1]}, G^{[P]}) \neq C_I(G^{[2]}, G^{[P]})$ (or $C_S(G^{[1]}, G^{[P]}) \neq C_S(G^{[2]}, G^{[P]})$), they can be distinguished by \mathcal{F} .*

What about the converse? When the space \mathcal{G} is finite, such as if the graphs have bounded numbers of nodes and the node as well as edge features belong to finite alphabets, we can show a slightly weaker statement than the exact converse. Following Chen et al. (2019b), we define an augmentation of families of functions using feed-forward neural networks as follows:

Definition 16. *Given \mathcal{F} , a family of functions from a space \mathcal{X} to \mathbb{R} , we consider an augmented family of functions also from \mathcal{X} to \mathbb{R} consisting of all functions of the following form*

$$x \mapsto h_{\mathcal{NN}}([f_1(x), \dots, f_d(x)]),$$

where $d \in \mathbb{N}$, $f_1, \dots, f_d \in \mathcal{F}$, and $h_{\mathcal{NN}}$ is a feed-forward neural network / multi-layer perceptron. When \mathcal{NN} is restricted to have L layers at most, we denote this augmented family by \mathcal{F}^{+L} .

Lemma 17. *Suppose \mathcal{X} is a finite space, g is a function mapping \mathcal{X} to \mathbb{R} , and \mathcal{F} is a family of functions mapping \mathcal{X} to \mathbb{R} . Then, \mathcal{F}^{+1} is able to approximate g on \mathcal{G} if $\forall x_1, x_2 \in \mathcal{X}$ with $g(x_1) \neq g(x_2)$, $\exists f \in \mathcal{F}$ such that $f(x_1) \neq f(x_2)$.*

Proof. Since \mathcal{X} is a finite space, for some large enough integer d , \exists a collection of d functions, $f_1, \dots, f_d \in \mathcal{F}$ such that, if we define the function $\mathbf{f}(x) = (f_1(x), \dots, f_d(x)) \in \mathbb{R}^d$, then it holds that $\forall x_1, x_2 \in \mathcal{X}, \mathbf{f}(x_1) = \mathbf{f}(x_2) \Rightarrow g(x_1) = g(x_2)$. (In fact, we can choose $d \leq \frac{|\mathcal{X}| \cdot (|\mathcal{X}| - 1)}{2}$, since in the worst case we need one f_i per pair of $x_1, x_2 \in \mathcal{X}$ with $x_1 \neq x_2$.) Then, \exists a well-defined function h from \mathbb{R}^d to \mathbb{R} such that $\forall x \in \mathcal{X}, g(x) = h(\mathbf{f}(x))$. By the universal approximation power of neural networks (Cybenko, 1989; Hornik, 1991), h can then be approximated arbitrarily well by some neural network $h_{\mathcal{NN}}$. \square

Thus, in the context of substructure counting, we have the following observation.

Observation 2. *Suppose \mathcal{G} is a finite space. If $\forall G^{[1]}, G^{[2]} \in \mathcal{G}$ with $C_I(G^{[1]}, G^{[P]}) \neq C_I(G^{[2]}, G^{[P]})$ (or $C_S(G^{[1]}, G^{[P]}) \neq C_S(G^{[2]}, G^{[P]})$), \mathcal{F} is able to distinguish $G^{[1]}$ and $G^{[2]}$, then \mathcal{F}^{+1} is able to approximate the induced-subgraph-count (or subgraph-count) function of the pattern $G^{[P]}$ on \mathcal{G} .*

For many GNN families, \mathcal{F}^{+1} in fact has the same expressive power as \mathcal{F} . For example, consider $\mathcal{F}_{\text{MPNN}}$, the family of all Message Passing Neural Networks on \mathcal{G} . $\mathcal{F}_{\text{MPNN}}^{+1}$ consists of functions that run several MPNNs on the input graph in parallel and stack their outputs to pass through an MLP. However, running several MPNNs in parallel is equivalent to running one MPNN with larger dimensions of hidden states and messages, and moreover the additional MLP at the end can be merged into the readout function. Similar holds for the family of all k -Invariant Graph Networks (k -IGNs). Hence, for such GNN families, we have an exact equivalence on finite graph spaces \mathcal{G} .

B Additional notations in the proofs

For two positive integers a and b , we define $\text{MOD}_a(b)$ to be a if a divides b and the number c such that $b \equiv c \pmod{a}$ otherwise. Hence the value ranges from 1 to a as we vary $b \in \mathbb{N}^*$.

For a positive integer c , let $[c]$ denote the set $\{1, \dots, c\}$.

Two k -tuples, $(i_1, \dots, i_k), (j_1, \dots, j_k) \in V^k$ are said to be in the same *equivalent class* if \exists a permutation π on V such that $(\pi(i_1), \dots, \pi(i_k)) = (j_1, \dots, j_k)$. Note that belonging to the same equivalence class is a weaker condition than having the same isomorphism type, as will be defined in Appendix C, which has to do with what the graphs look like.

For any k -tuple, $s = (i_1, \dots, i_k)$, and for $w \in [k]$, use $I_w(s)$ to denote the w th entry of s , i_w .

C Definition of k -WL on attributed graphs

In this Section we introduce the general k -WL test for $k \in \mathbb{N}^*$ applied to a pair of graphs, $G^{[1]}$ and $G^{[2]}$. Assume that the two graphs have the same number of vertices, since otherwise they can be told apart easily. Without loss of generality, we assume that they share the same set of vertex indices, V (but can differ in E , x or e). For each of the graphs, at iteration 0, the test assigns an initial color in some color space to every k -tuple in V^k according to its isomorphism type (we define isomorphism types rigorously in Section C.1), and then updates the coloring in every iteration. For any k -tuple $s = (i_1, \dots, i_k) \in V^k$, we let $\mathbf{c}_k^{(t)}(s)$ denote the color of s in $G^{[1]}$ assigned at t th iteration, and let $\mathbf{c}'_k^{(t)}(s)$ denote the color it receives in $G^{[2]}$. $\mathbf{c}_k^{(t)}(s)$ and $\mathbf{c}'_k^{(t)}(s)$ are updated iteratively as follows. For each $w \in [k]$, define the neighborhood

$$N_w(s) = \{(i_1, \dots, i_{w-1}, j, i_{w+1}, \dots, i_k) : j \in V\}$$

Given $\mathbf{c}_k^{(t-1)}$ and $\mathbf{c}'_k^{(t-1)}$, define

$$\begin{aligned} C_w^{(t)}(s) &= \text{HASH}_{t,1} \left(\{ \mathbf{c}_k^{(t-1)}(\tilde{s}) : \tilde{s} \in N_w(s) \} \right) \\ C'_w{}^{(t)}(s) &= \text{HASH}_{t,1} \left(\{ \mathbf{c}'_k{}^{(t-1)}(\tilde{s}) : \tilde{s} \in N_w(s) \} \right) \end{aligned}$$

with “ $\{\}$ ” representing a multiset, and $\text{HASH}_{t,1}$ being some hash function that maps injectively from the space of multisets of colors to some intermediate space. Then let

$$\begin{aligned} \mathbf{c}_k^{(t)}(s) &= \text{HASH}_{t,2} \left(\left(\mathbf{c}_k^{(t-1)}(s), \left(C_1^{(t)}(s), \dots, C_k^{(t)}(s) \right) \right) \right) \\ \mathbf{c}'_k^{(t)}(s) &= \text{HASH}_{t,2} \left(\left(\mathbf{c}'_k^{(t-1)}(s), \left(C'_1{}^{(t)}(s), \dots, C'_k{}^{(t)}(s) \right) \right) \right) \end{aligned}$$

where $\text{HASH}_{t,2}$ maps injectively from its input space to the space of colors. The test will terminate and return the result that the two graphs are not isomorphic if at some iteration t , the following two multisets differ:

$$\{\mathbf{c}_k^{(t)}(s) : s \in V^k\} \neq \{\mathbf{c}'_k^{(t)}(s) : s \in V^k\}$$

C.1 Isomorphism types of k -tuples in k -WL for attributed graphs

Say $G^{[1]} = (V^{[1]}, E^{[1]}, x^{[1]}, e^{[1]})$, $G^{[2]} = (V^{[2]}, E^{[2]}, x^{[2]}, e^{[2]})$.

a) $\forall s = (i_1, \dots, i_k), s' = (i'_1, \dots, i'_k) \in (V^{[1]})^k$, s and s' are said to have the same isomorphism type if

1. $\forall \alpha, \beta \in [k], i_\alpha = i_\beta \Leftrightarrow i'_\alpha = i'_\beta$
2. $\forall \alpha \in [k], x_{i_\alpha}^{[1]} = x_{i'_\alpha}^{[1]}$
3. $\forall \alpha, \beta \in [k], (i_\alpha, i_\beta) \in E^{[1]} \Leftrightarrow (i'_\alpha, i'_\beta) \in E^{[1]}$, and moreover, if either side is true, then $e_{i_\alpha, i_\beta}^{[1]} = e_{i'_\alpha, i'_\beta}^{[1]}$

b) Similar if both $s, s' \in (V^{[2]})^k$.

c) $\forall s = (i_1, \dots, i_k) \in (V^{[1]})^k, s' = (i'_1, \dots, i'_k) \in (V^{[2]})^k$, s and s' are said to have the same isomorphism type if

1. $\forall \alpha, \beta \in [k], i_\alpha = i_\beta \Leftrightarrow i'_\alpha = i'_\beta$
2. $\forall \alpha \in [k], x_{i_\alpha}^{[1]} = x_{i'_\alpha}^{[2]}$
3. $\forall \alpha, \beta \in [k], (i_\alpha, i_\beta) \in E^{[1]} \Leftrightarrow (i'_\alpha, i'_\beta) \in E^{[2]}$, and moreover, if either side is true, then $e_{i_\alpha, i_\beta}^{[1]} = e_{i'_\alpha, i'_\beta}^{[2]}$

In k -WL tests, two k -tuples s and s' in either $(V^{[1]})^k$ or $(V^{[2]})^k$ are assigned the same color at iteration 0 if and only if they have the same isomorphism type.

For a reference, see [Maron et al. \(2019b\)](#).

D Proof of Lemma 2 (MPNNs are no more powerful than 2-WL)

Proof. Suppose for contradiction that there exists an MPNN with T_0 layers that can distinguish the two graphs. Let $m^{(t)}$ and $h^{(t)}$, $m'^{(t)}$ and $h'^{(t)}$ be the messages and hidden states at layer t obtained

by applying the MPNN on the two graphs, respectively. Define

$$\tilde{h}_{i,j}^{(t)} = \begin{cases} h_i^{(t)} & \text{if } i = j \\ \left(h_i^{(t)}, h_j^{(t)}, a_{i,j}, e_{i,j} \right) & \text{otherwise} \end{cases}$$

$$\tilde{h}'_{i,j}{}^{(t)} = \begin{cases} h'_i{}^{(t)} & \text{if } i = j \\ \left(h'_i{}^{(t)}, h'_j{}^{(t)}, a'_{i,j}, e'_{i,j} \right) & \text{otherwise,} \end{cases}$$

where $a_{i,j} = 1$ if $(i,j) \in E^{[1]}$ and 0 otherwise, $e_{i,j} = e_{i,j}^{[1]}$ is the edge feature of the first graph, and a', e' are defined similarly for the second graph.

Since the two graphs cannot be distinguished by 2-WL, then for the T_0 th iteration, there is

$$\{\mathbf{c}_2^{(T_0)}(s) : s \in V^2\} = \{\mathbf{c}'_2{}^{(T_0)}(s) : s \in V^2\},$$

which implies that there exists a permutation on V^2 , which we can call η_0 , such that $\forall s \in V^2$, there is $\mathbf{c}_2^{(T_0)}(s) = \mathbf{c}'_2{}^{(T_0)}(\eta_0(s))$. To take advantage of this condition, we introduce the following lemma, which is central to the proof.

Lemma 18. $\forall t \leq T_0, \forall i, j, i', j' \in V$, if $\mathbf{c}_2^{(t)}((i, j)) = \mathbf{c}'_2{}^{(t)}((i', j'))$, then

1. $i = j \Leftrightarrow i' = j'$.
2. $\tilde{h}_{i,j}^{(t)} = \tilde{h}'_{i',j'}{}^{(t)}$

Proof of Lemma 18: First, we state the following simple observation without proof, which is immediate given the update rule of k -WL:

Lemma 19. For k -WL, $\forall s, s' \in V^k$, if for some t_0 , $\mathbf{c}_k^{(t_0)}(s) = \mathbf{c}'_k{}^{(t_0)}(s')$, then $\forall t \in [0, t_0]$, $\mathbf{c}_k^{(t)}(s) = \mathbf{c}'_k{}^{(t)}(s')$.

For the first condition, assuming $\mathbf{c}_2^{(t)}((i, j)) = \mathbf{c}'_2{}^{(t)}((i', j'))$, Lemma 19 then tells us that $\mathbf{c}_2^{(0)}((i, j)) = \mathbf{c}'_2{}^{(0)}((i', j'))$. Since the colors in 2-WL are initialized by the isomorphism type of the node pair, it has to be that $i = j \Leftrightarrow i' = j'$.

We will prove the second condition by induction on t . For the base case, $t = 0$, we want to show that $\forall i, j, i', j' \in V$, if $\mathbf{c}_2^{(0)}((i, j)) = \mathbf{c}'_2{}^{(0)}((i', j'))$ then $\tilde{h}_{i,j}^{(0)} = \tilde{h}'_{i',j'}{}^{(0)}$. If $i = j$, then $\mathbf{c}_2^{(0)}((i, i)) = \mathbf{c}'_2{}^{(0)}((i', i'))$ if and only if $x_i = x'_{i'}$, which is equivalent to $h_i^{(0)} = h'_{i'}{}^{(0)}$, and hence $\tilde{h}_i^{(0)} = \tilde{h}'_{i'}{}^{(0)}$. If $i \neq j$, then by the definition of isomorphism types given in Appendix C, $\mathbf{c}_2^{(0)}((i, j)) = \mathbf{c}'_2{}^{(0)}((i', j'))$ implies that

$$\begin{aligned} x_i = x'_{i'} &\Rightarrow h_i^{(0)} = h'_{i'}{}^{(0)} \\ x_j = x'_{j'} &\Rightarrow h_j^{(0)} = h'_{j'}{}^{(0)} \\ a_{i,j} &= a'_{i',j'} \\ e_{i,j} &= e'_{i',j'} \end{aligned}$$

which yields $\tilde{h}_{i,j}^{(0)} = \tilde{h}'_{i',j'}{}^{(0)}$.

Next, to prove the inductive step, assume that for some $T \in [T_0]$, the statement in Lemma 18 holds for all $t \leq T - 1$, and consider $\forall i, j, i', j' \in V$ such that $\mathbf{c}_2^{(T)}((i, j)) = \mathbf{c}'_2{}^{(T)}((i', j'))$. By the update

rule of 2-WL, this implies that

$$\begin{aligned}
\mathbf{c}_2^{(T-1)}((i, j)) &= \mathbf{c}'_2{}^{(T-1)}((i', j')) \\
\{\mathbf{c}_2^{(T-1)}((k, j)) : k \in V\} &= \{\mathbf{c}'_2{}^{(T-1)}((k, j')) : k \in V\} \\
\{\mathbf{c}_2^{(T-1)}((i, k)) : k \in V\} &= \{\mathbf{c}'_2{}^{(T-1)}((i', k)) : k \in V\}
\end{aligned} \tag{3}$$

The first condition, thanks to the inductive hypothesis, implies that $\tilde{h}_{i,j}^{(T-1)} = \tilde{h}'_{i',j'}{}^{(T-1)}$. In particular, if $i \neq j$, then we have

$$\begin{aligned}
a_{i,j} &= a'_{i',j'} \\
e_{i,j} &= e'_{i',j'}
\end{aligned} \tag{4}$$

The third condition implies that \exists a permutation on V , which we can call $\xi_{i,i'}$, such that $\forall k \in V$,

$$\mathbf{c}_2^{(T-1)}((i, k)) = \mathbf{c}'_2{}^{(T-1)}((i', \xi_{i,i'}(k)))$$

By the inductive hypothesis, there is $\forall k \in V$,

$$\tilde{h}_{i,k}^{(T-1)} = \tilde{h}'_{i',\xi_{i,i'}(k)}{}^{(T-1)}$$

and moreover, $\xi_{i,i'}(k) = i'$ if and only if $k = i$. For $k \neq i$, we thus have

$$\begin{aligned}
h_i^{(T-1)} &= h'_{i'}{}^{(T-1)} \\
h_k^{(T-1)} &= h'_{\xi_{i,i'}(k)}{}^{(T-1)} \\
a_{i,k} &= a'_{i',\xi_{i,i'}(k)} \\
e_{i,k} &= e'_{i',\xi_{i,i'}(k)}
\end{aligned}$$

Now, looking at the update rule at the T th layer of the MPNN,

$$\begin{aligned}
m_i^{(T)} &= \sum_{k \in \mathcal{N}(i)} M_T(h_i^{(T-1)}, h_k^{(T-1)}, e_{i,k}) \\
&= \sum_{k \in V} a_{i,k} \cdot M_T(h_i^{(T-1)}, h_k^{(T-1)}, e_{i,k}) \\
&= \sum_{k \in V} a'_{i',\xi_{i,i'}(k)} \cdot M_T(h'_{i'}{}^{(T-1)}, h'_{\xi_{i,i'}(k)}{}^{(T-1)}, e'_{i',\xi_{i,i'}(k)}) \\
&= \sum_{k' \in V} a'_{i',k'} \cdot M_T(h'_{i'}{}^{(T-1)}, h'_{k'}{}^{(T-1)}, e'_{i',k'}) \\
&= m'_{i'}{}^{(T)}
\end{aligned}$$

where between the third and the fourth line we made the substitution $k' = \xi_{i,i'}(k)$. Therefore,

$$\begin{aligned}
h_i^{(T)} &= U_i(h_i^{(T-1)}, m_i^{(T)}) \\
&= U_i(h'_{i'}{}^{(T-1)}, m'_{i'}{}^{(T)}) \\
&= h'_{i'}{}^{(T)}
\end{aligned}$$

By the symmetry between i and j , we can also show that $h_j^{(T)} = h'_{j'}{}^{(T)}$. Hence, together with 4, we can conclude that

$$\tilde{h}_{i,j}^{(T)} = \tilde{h}'_{i',j'}{}^{(T)}$$

which proves the lemma. \square

Thus, the second result of this lemma tells us that $\forall i, j \in V^2$, $\tilde{h}_{i,j}^{(T_0)} = \tilde{h}_{\eta_0(i,j)}^{(T_0)}$. Moreover, by the first result, \exists a permutation on V , which we can call τ_0 , such that $\forall i \in V$, $\eta((i, i)) = (\tau_0(i), \tau_0(i))$. Combining the two, we have that $\forall i \in V$, $h_i^{(T_0)} = h_{\tau(i)}^{(T_0)}$, and hence

$$\{h_i^{(T_0)} : i \in V\} = \{h_{i'}^{(T_0)} : i' \in V\} \quad (5)$$

Therefore, $\hat{y} = \hat{y}'$, meaning that the MPNN returns identical outputs on the two graphs. \square

E Proof of Theorem 3 (2-WL is unable to induced-subgraph-count patterns of 3 or more nodes)

Proof Intuition. Given any connected pattern of at least 3 nodes, such as the one drawn in Figure 1, we can construct a pair of graphs, such as the ones drawn in Figure 2. They that have different induced-subgraph-counts of the pattern, and we can show that 2-WL cannot distinguish them. but cannot be distinguished from each other by 2-WL. For instance, if we run 2-WL on the pair of graphs in Figure 2, then there will be $\mathbf{c}_2^{(t)}((1, 3)) = \mathbf{c}'_2^{(t)}((1, 3))$, $\mathbf{c}_2^{(t)}((1, 2)) = \mathbf{c}'_2^{(t)}((1, 6))$, $\mathbf{c}_2^{(t)}((1, 6)) = \mathbf{c}'_2^{(t)}((1, 2))$, and so on. We can in fact show that $\{\mathbf{c}_2^{(t)}(s) : s \in V^2\} = \{\mathbf{c}'_2^{(t)}(s) : s \in V^2\}, \forall t$, which implies that 2-WL cannot distinguish the two graphs.

Proof. Say $G^{[P]} = (V^{[P]}, E^{[P]}, x^{[P]}, e^{[P]})$ is a connected pattern of m nodes, where $m > 2$, and thus $V^{[P]} = [m]$.

First, if $G^{[P]}$ is not a clique, then by definition, there exists two distinct nodes $i, j \in V^{[P]}$ such that i and j are not connected by an edge. Assume without loss of generality that $i = 1$ and $j = 2$. Now, construct two graphs $G^{[1]} = (V = [2m], E^{[1]}, x^{[1]}, e^{[1]})$, $G^{[2]} = (V = [2m], E^{[2]}, x^{[2]}, e^{[2]})$ both with $2m$ nodes. For $G^{[1]}$, let $E^{[1]} = \{(i, j) : i, j \leq m, (i, j) \in E^{[P]}\} \cup \{(i + m, j + m) : i, j \leq m, (i, j) \in E^{[P]}\} \cup \{(1, 2), (2, 1), (1 + m, 2 + m), (2 + m, 1 + m)\}$; $\forall i \leq m, x_i^{[1]} = x_{i+m}^{[1]} = x_i^{[P]}$; $\forall (i, j) \in E^{[P]}, e_{i,j}^{[1]} = e_{i+m,j+m}^{[1]} = e_{i,j}^{[P]}$, and moreover we can randomly choose a value of edge feature for $e_{1,2}^{[1]} = e_{2,1}^{[1]} = e_{1+m,2+m}^{[1]} = e_{2+m,1+m}^{[1]}$. For $G^{[2]}$, let $E^{[2]} = \{(i, j) : i, j \leq m, (i, j) \in E^{[P]}\} \cup \{(i + m, j + m) : i, j \leq m, (i, j) \in E^{[P]}\} \cup \{(1, 2 + m), (2 + m, 1), (1 + m, 2), (2, 1 + m)\}$; $\forall i \leq m, x_i^{[2]} = x_{i+m}^{[2]} = x_i^{[P]}$; $\forall (i, j) \in E^{[P]}, e_{i,j+m}^{[2]} = e_{i+m,j}^{[2]} = e_{i,j}^{[P]}$, and moreover we let $e_{1,2+m}^{[2]} = e_{2+m,1}^{[2]} = e_{1+m,2}^{[2]} = e_{2,1+m}^{[2]} = e_{1,2}^{[1]}$. In words, both $G^{[1]}$ and $G^{[2]}$ are constructed based on two copies of $G^{[P]}$, and the difference is that, $G^{[1]}$ adds the edges $\{(1, 2), (2, 1), (1 + m, 2 + m), (2 + m, 1 + m)\}$, whereas $G^{[2]}$ adds the edges $\{(1, 2 + m), (2 + m, 1), (1 + m, 2), (2, 1 + m)\}$, all with the same edge feature.

On one hand, by construction, 2-WL will not be able to distinguish $G^{[1]}$ from $G^{[2]}$. This is intuitive if we compare the rooted subtrees in the two graphs, as there exists a bijection from $V^{[1]}$ to $V^{[2]}$ that preserves the rooted subtree structure. A rigorous proof is given at the end of this section. In addition, we note that this is also consequence of the direct proof of Corollary 13 given in Appendix J, in which we will show that the same pair of graphs cannot be distinguished by 2-IGNs. Since 2-IGNs are no less powerful than 2-WL (Maron et al., 2019b), this implies that 2-WL cannot distinguish them either.

On the other hand, $G^{[1]}$ and $G^{[2]}$ has different matching-count of the pattern. $G^{[1]}$ contains no subgraph isomorphic to $G^{[P]}$. Intuitively this is obvious; to be rigorous, note that firstly, neither the subgraph induced by the nodes $\{1, \dots, m\}$ nor the subgraph induced by the nodes $\{1 + m, \dots, 2m\}$ is isomorphic to $G^{[P]}$, and secondly, the subgraph induced by any other set of m nodes is not connected, whereas $G^{[P]}$ is connected. $G^{[2]}$, however, has at least two induced subgraphs isomorphic to $G^{[P]}$, one

induced by the nodes $\{1, \dots, m\}$, and the other induced by the nodes $\{1 + m, \dots, 2m\}$.

If $G^{[P]}$ is a clique, then we also first construct $G^{[1]}$, $G^{[2]}$ from $G^{[P]}$ as two copies of $G^{[P]}$. Then, for $G^{[1]}$, we pick two distinct nodes $1, 2 \in V^{[P]}$ and remove the edges $(1, 2)$, $(2, 1)$, $(1 + m, 2 + m)$ and $(2 + m, 1 + m)$ from $V^{[1]}$, while adding edges $(1, 2 + m)$, $(2 + m, 1)$, $(1 + m, 2)$, $(2, 1 + m)$ with the same edge features. Then, $G^{[1]}$ contains no subgraph isomorphic to $G^{[P]}$, while $G^{[2]}$ contains two. Note that the pair of graphs is the same as the counterexample pair of graphs that could have been constructed in the non-clique case for the pattern that is a clique with one edge deleted. Hence 2-WL still cant distinguish $G^{[1]}$ from $G^{[2]}$. \square

Proof of 2-WL failing to distinguish $G^{[1]}$ and $G^{[2]}$:

To show that 2-WL cannot distinguish $G^{[1]}$ from $G^{[2]}$, we need to show that if we run 2-WL on the two graphs, then $\forall T, \{\mathbf{c}^{(T)}((i, j)) : i, j \in V\} = \{\mathbf{c}'^{(T)}((i, j)) : i, j \in V\}$. For this to hold, it is sufficient to find a bijective map $\eta : V^2 \rightarrow V^2$ such that $\mathbf{c}^{(T)}((i, j)) = \mathbf{c}'^{(T)}(\eta((i, j)))$, $\forall i, j \in V$. First, we define a set $S = \{(1, 2), (2, 1), (1 + m, 2 + m), (2 + m, 1 + m), (1, 2 + m), (2 + m, 1), (1 + m, 2), (2, 1 + m)\}$, which represents the “special” pairs of nodes that capture the difference between $G^{[1]}$ and $G^{[2]}$. Then we can define $\eta : V^2 \rightarrow V^2$ as

$$\eta((i, j)) = \begin{cases} (i, j), & \text{if } (i, j) \notin S \\ (i, \text{MOD}_{2m}(j + m)), & \text{if } (i, j) \in S \end{cases}$$

Note that η is a bijective. It is easy to verify that η is a color-preserving map between node pairs in $G^{[1]}$ and node pairs in $G^{[2]}$ at initialization, i.e. $\mathbf{c}^{(0)}((i, j)) = \mathbf{c}'^{(0)}(\eta((i, j)))$, $\forall i, j \in V$. We will prove by induction that in fact it remains such a color-preserving map at any iteration T . The inductive step that we need to prove is,

Lemma 20. *For any positive integer t , supposing that $\mathbf{c}^{(t-1)}((i, j)) = \mathbf{c}'^{(t-1)}(\eta((i, j)))$, $\forall i, j \in V$, then we also have $\mathbf{c}^{(t)}((i, j)) = \mathbf{c}'^{(t)}(\eta((i, j)))$, $\forall i, j \in V$.*

Proof of Lemma 20: By the update rule of 2-WL, $\forall i, j \in V$, to show that $\mathbf{c}^{(t)}((i, j)) = \mathbf{c}'^{(t)}(\eta((i, j)))$, we need to establish three conditions:

$$\mathbf{c}^{(t-1)}((i, j)) = \mathbf{c}'^{(t-1)}(\eta((i, j))) \tag{6}$$

$$\{\mathbf{c}^{(t-1)}(\tilde{s}) : \tilde{s} \in N_1((i, j))\} = \{\mathbf{c}'^{(t-1)}(\tilde{s}) : \tilde{s} \in N_1(\eta((i, j)))\} \tag{7}$$

$$\{\mathbf{c}^{(t-1)}(\tilde{s}) : \tilde{s} \in N_2((i, j))\} = \{\mathbf{c}'^{(t-1)}(\tilde{s}) : \tilde{s} \in N_2(\eta((i, j)))\} \tag{8}$$

The first condition is already guaranteed by the inductive hypothesis. Now we prove the last two conditions by examining different cases separately below.

Case 1 $i, j \notin \{1, 2, 1 + m, 2 + m\}$

Then $\eta((i, j)) = (i, j)$, and $N_1((i, j)) \cap S = \emptyset$, $N_2((i, j)) \cap S = \emptyset$. Therefore, η restricted to $N_1((i, j))$ or $N_2((i, j))$ is the identity map, and thus

$$\begin{aligned} \{\mathbf{c}^{(t-1)}(\tilde{s}) : \tilde{s} \in N_1((i, j))\} &= \{\mathbf{c}'^{(t-1)}(\eta(\tilde{s})) : \tilde{s} \in N_1((i, j))\} \\ &= \{\mathbf{c}'^{(t-1)}(\tilde{s}) : \tilde{s} \in N_1(\eta((i, j)))\}, \end{aligned}$$

thanks to the inductive hypothesis. Similar for the condition (8).

Case 2 $i \in \{1, 1+m\}, j \notin \{1, 2, 1+m, 2+m\}$

Then $\eta((i, j)) = (i, j)$, $N_2((i, j)) \cap S = \{(i, 2), (i, 2+m)\}$, and $N_1((i, j)) \cap S = \emptyset$. To show condition (8), note that η is the identity map when restricted to $N_2((i, j)) \setminus \{(i, 2), (i, 2+m)\}$, and hence

$$\{\mathbf{c}^{(t-1)}(\tilde{s}) : \tilde{s} \in N_2((i, j)) \setminus \{(i, 2), (i, 2+m)\}\} = \{\mathbf{c}'^{(t-1)}(\tilde{s}) : \tilde{s} \in N_2((i, j)) \setminus \{(i, 2), (i, 2+m)\}\}$$

Moreover, $\eta((i, 2)) = (i, 2+m)$ and $\eta((i, 2+m)) = (i, 2)$. Hence, by the inductive hypothesis, $\mathbf{c}^{(t-1)}((i, 2)) = \mathbf{c}'^{(t-1)}((i, 2+m))$ and $\mathbf{c}^{(t-1)}((i, 2+m)) = \mathbf{c}'^{(t-1)}((i, 2))$. Therefore,

$$\begin{aligned} \{\mathbf{c}^{(t-1)}(\tilde{s}) : \tilde{s} \in N_2((i, j))\} &= \{\mathbf{c}'^{(t-1)}(\tilde{s}) : \tilde{s} \in N_2((i, j))\} \\ &= \{\mathbf{c}'^{(t-1)}(\tilde{s}) : \tilde{s} \in N_2(\eta((i, j)))\}, \end{aligned}$$

which shows condition (8). Condition (7) is easily seen as η restricted to $N_1((i, j))$ is the identity map.

Case 3 $j \in \{1, 1+m\}, i \notin \{1, 2, 1+m, 2+m\}$

There is $\eta((i, j)) = (i, j)$, $N_1((i, j)) \cap S = \{(2, j), (2+m, j)\}$, and $N_2((i, j)) \cap S = \emptyset$. Hence the proof can be carried out analogously to case 2.

Case 4 $i \in \{2, 2+m\}, j \notin \{1, 2, 1+m, 2+m\}$

There is $\eta((i, j)) = (i, j)$, $N_2((i, j)) \cap S = \{(i, 1), (i, 1+m)\}$, and $N_1((i, j)) \cap S = \emptyset$. Hence the proof can be carried out analogously to case 2.

Case 5 $j \in \{2, 2+m\}, i \notin \{1, 2, 1+m, 2+m\}$

There is $\eta((i, j)) = (i, j)$, $N_1((i, j)) \cap S = \{(1, j), (1+m, j)\}$, and $N_2((i, j)) \cap S = \emptyset$. Hence the proof can be carried out analogously to case 2.

Case 6 $(i, j) \in S$

There is $\eta((i, j)) = (i, \text{MOD}_{2m}(j))$, $N_1((i, j)) \cap S = \{(i, j), (\text{MOD}_{2m}(i), j)\}$, $N_2((i, j)) \cap S = \{(i, j), (i, \text{MOD}_{2m}(j))\}$. Thus, $N_1(\eta((i, j))) = N_1((i, \text{MOD}_{2m}(j)))$, $N_2(\eta((i, j))) = N_2((i, \text{MOD}_{2m}(j))) = N_2((i, j))$. Once again, η is the identity map when restricted to $N_1((i, j)) \setminus S$ or $N_2((i, j)) \setminus S$. Hence, by the inductive hypothesis, there is

$$\{\mathbf{c}^{(t-1)}(\tilde{s}) : \tilde{s} \in N_1((i, j)) \setminus \{(i, j), (\text{MOD}_{2m}(i), j)\}\} = \{\mathbf{c}'^{(t-1)}(\tilde{s}) : \tilde{s} \in N_1((i, j)) \setminus \{(i, j), (\text{MOD}_{2m}(i), j)\}\}$$

$$\{\mathbf{c}^{(t-1)}(\tilde{s}) : \tilde{s} \in N_2((i, j)) \setminus \{(i, j), (i, \text{MOD}_{2m}(j))\}\} = \{\mathbf{c}'^{(t-1)}(\tilde{s}) : \tilde{s} \in N_2((i, j)) \setminus \{(i, j), (i, \text{MOD}_{2m}(j))\}\}$$

Also from the inductive hypothesis, we have

$$\begin{aligned} \mathbf{c}^{(t-1)}((i, j)) &= \mathbf{c}'^{(t-1)}(\eta((i, j))) \\ &= \mathbf{c}'^{(t-1)}((i, \text{MOD}_{2m}(j))), \end{aligned} \tag{9}$$

$$\begin{aligned} \mathbf{c}^{(t-1)}((i, j)) &= \mathbf{c}^{(t-1)}((j, i)) \\ &= \mathbf{c}'^{(t-1)}(\eta((j, i))) \\ &= \mathbf{c}'^{(t-1)}((j, \text{MOD}_{2m}(i))) \\ &= \mathbf{c}'^{(t-1)}((\text{MOD}_{2m}(i), j)), \end{aligned} \tag{10}$$

$$\begin{aligned} \mathbf{c}^{(t-1)}((i, \text{MOD}_{2m}(j))) &= \mathbf{c}'^{(t-1)}(\eta((i, \text{MOD}_{2m}(j)))) \\ &= \mathbf{c}'^{(t-1)}((i, \text{MOD}_{2m}(\text{MOD}_{2m}(j)))) \\ &= \mathbf{c}'^{(t-1)}((i, j)), \end{aligned} \tag{11}$$

$$\begin{aligned}
\mathbf{c}^{(t-1)}((\text{MOD}_{2m}(i), j)) &= \mathbf{c}^{(t-1)}((j, \text{MOD}_{2m}(i))) \\
&= \mathbf{c}'^{(t-1)}(\eta((j, \text{MOD}_{2m}(i)))) \\
&= \mathbf{c}'^{(t-1)}((j, \text{MOD}_{2m}(\text{MOD}_{2m}(i)))) \\
&= \mathbf{c}'^{(t-1)}((j, i)) \\
&= \mathbf{c}'^{(t-1)}((i, j)),
\end{aligned} \tag{12}$$

where in (10) and (12), the first and the last equalities are thanks to the symmetry of the coloring between any pair of nodes (i', j') and its “reversed” version (j', i') , which persists throughout all iterations, as well as the fact that if $(i', j') \in S$, then $(j', i') \in S$. Therefore, we now have

$$\{\mathbf{c}^{(t-1)}(\tilde{s}) : \tilde{s} \in N_1((i, j))\} = \{\mathbf{c}'^{(t-1)}(\tilde{s}) : \tilde{s} \in N_1((i, j))\} \tag{13}$$

$$\{\mathbf{c}^{(t-1)}(\tilde{s}) : \tilde{s} \in N_2((i, j))\} = \{\mathbf{c}'^{(t-1)}(\tilde{s}) : \tilde{s} \in N_2((i, j))\} \tag{14}$$

Since $\eta((i, j)) = (i, \text{MOD}_{2m}(j))$, we have

$$\begin{aligned}
N_1(\eta((i, j))) &= \{(k, \text{MOD}_{2m}(j)) : k \in V\} \\
&= \{(k, \text{MOD}_{2m}(j)) : (\text{MOD}_{2m}(k), j) \in N_1((i, j))\} \\
&= \{(\text{MOD}_{2m}(k), \text{MOD}_{2m}(j)) : (k, j) \in N_1((i, j))\}
\end{aligned}$$

Thanks to the symmetry of the coloring under the map $(i', j') \rightarrow (\text{MOD}_{2m}(i'), \text{MOD}_{2m}(j'))$, we then have

$$\begin{aligned}
\{\mathbf{c}'^{(t-1)}(\tilde{s}) : \tilde{s} \in N_1(\eta((i, j)))\} &= \{\mathbf{c}'^{(t-1)}((\text{MOD}_{2m}(k), \text{MOD}_{2m}(j)) : (k, j) \in N_1((i, j)))\} \\
&= \{\mathbf{c}'^{(t-1)}((k, j)) : (k, j) \in N_1((i, j))\} \\
&= \{\mathbf{c}'^{(t-1)}(\tilde{s}) : \tilde{s} \in N_1((i, j))\}
\end{aligned}$$

Therefore, combined with (13), we see that (7) is proved. (8) is a straightforward consequence of (14), since $N_2((i, j)) = N_2(\eta((i, j)))$.

Case 7 $i, j \in \{1, 1+m\}$

There is $\eta((i, j)) = (i, j)$, $N_2((i, j)) \cap S = \{(i, 2), (i, 2+m)\}$, and $N_1((i, j)) \cap S = \{(2, j), (2+m, j)\}$. Thus, both (7) and (8) can be proved analogously to how (8) is proved for case 2.

Case 8 $i, j \in \{2, 2+m\}$

There is $\eta((i, j)) = (i, j)$, $N_2((i, j)) \cap S = \{(i, 1), (i, 1+m)\}$, and $N_1((i, j)) \cap S = \{(1, j), (1+m, j)\}$. Thus, both (7) and (8) can be proved analogously to how (8) is proved for case 2.

With conditions (7) and (8) shown for all pairs of $(i, j) \in V^2$, we know that by the update rules of 2-WL, there is $\mathbf{c}^{(t)}((i, j)) = \mathbf{c}'^{(t)}(\eta((i, j)))$, $\forall i, j \in V$. □

With Lemma 20 justifying the inductive step, we see that for any positive integer T , there is $\mathbf{c}^{(T)}((i, j)) = \mathbf{c}'^{(T)}(\eta((i, j)))$, $\forall i, j \in V$. Hence, we can conclude that $\forall T, \{\mathbf{c}^{(T)}((i, j)) : i, j \in V\} = \{\mathbf{c}'^{(T)}((i, j)) : i, j \in V\}$, which implies that the two graphs cannot be distinguished by 2-WL. □

F Proof of Theorem 5 (MPNNs are able to subgraph-count star-shaped patterns)

(See Section 2.1 of Arvind et al. (2018) for a proof for the case where all nodes have identical features.)

Proof. Without loss of generality, we represent a star-shaped pattern by $G^{[P]} = (V^{[P]}, E^{[P]}, x^{[P]}, e^{[P]})$, where $V^{[P]} = [m]$ (with node 1 representing the center) and $E^{[P]} = \{(1, i) : 2 \leq i \leq m\} \cup \{(i, 1) : 2 \leq i \leq m\}$.

Given a graph G , for each of its node j , we define $N(j)$ as the set of its neighbors in the graph. Then the neighborhood centered at j contributes to $C_S(G, G^{[P]})$ if and only if $x_j = x_1^{[P]}$ and $\exists S \subseteq N(j)$ such that the multiset $\{(x_k, e_{jk}) : k \in S\}$ equals the multiset $\{(x_k^{[P]}, e_{1k}^{[P]}) : 2 \leq k \leq m\}$. Moreover, the contribution to the number $C_S(G, G^{[P]})$ equals the number of all such subsets $S \subseteq N(j)$. Hence, we have the following decomposition

$$C_S(G, G^{[P]}) = \sum_{j \in V} f^{[P]}(x_j, \{(x_k, e_{jk}) : k \in N(j)\}),$$

where $f^{[P]}$, is defined for every 2-tuple consisting of a node feature and a multiset of pairs of node feature and edge feature (i.e., objects of the form

$$(x, M = \{(x_\alpha, e_\alpha) : \alpha \in K\})$$

where K is a finite set of indices) as

$$f^{[P]}(x, M) = \begin{cases} 0 & \text{if } x \neq x_1^{[P]} \\ \#_M^{[P]} & \text{if } x = x_1^{[P]} \end{cases}$$

where $\#_M^{[P]}$ denotes the number of sub-multisets of M that equals the multiset $\{(x_k^{[P]}, e_{1k}^{[P]}) : 2 \leq k \leq m\}$.

Thanks to Corollary 6 of [Xu et al. \(2018a\)](#) based on [Zaheer et al. \(2017\)](#), we know that $f^{[P]}$ can be expressed by some message-passing function in an MPNN. Thus, together with summation as the readout function, MPNN is able to express $C_S(G, G^{[P]})$. \square

G Proof of Theorem 7 (k -WL is able to count patterns of k or fewer nodes)

Proof. Suppose we run k -WL on two graphs, $G^{[1]}$ and $G^{[2]}$. In k -WL, the colorings of the k -tuples are initialized according to their isomorphism types as defined in Appendix C. Thus, if for some pattern of no more than k nodes, $G^{[1]}$ and $G^{[2]}$ have different matching-count or containment-count, then there exists an isomorphism type of k -tuples such that $G^{[1]}$ and $G^{[2]}$ differ in the number of k -tuples under this type. This implies that $\{\mathbf{c}_k^{(0)}(s) : s \in (V^{[1]})^k\} \neq \{\mathbf{c}'_k^{(0)}(s') : s' \in (V^{[2]})^k\}$, and hence the two graphs can be distinguished at the 0th iteration of k -WL. \square

H Proof of Theorem 9 (T iterations of k -WL cannot induced-subgraph-count path patterns of size $(k+1)2^T$ or more)

Proof. For any integer $m \geq (k+1)2^T$, we will construct two graphs $G^{[1]} = (V^{[1]} = [2m], E^{[1]}, x^{[1]}, e^{[1]})$ and $G^{[2]} = (V^{[2]} = [2m], E^{[2]}, x^{[2]}, e^{[2]})$, both with $2m$ nodes but with different matching-counts of H_m , and show that k -WL cannot distinguish them. Define $E_{double} = \{(i, i+1) : 1 \leq i < m\} \cup \{(i+1, i) : 1 \leq i < m\} \cup \{(i+m, i+m+1) : 1 \leq i < m\} \cup \{(i+m+1, i+m) : 1 \leq i < m\}$, which is the edge set of a graph that is exactly two disconnected copies of H_m . For $G^{[1]}$, let $E^{[1]} = E_{double} \cup \{(1, m), (m, 1), (1+m, 2m), (2m, 1+m)\}$; $\forall i \leq m, x_i^{[1]} = x_{i+m}^{[1]} = x_i^{[H_m]}$; $\forall (i, j) \in E^{[H_m]}, e_{j,i}^{[1]} = e_{j,i}^{[H_m]} = e_{i+m, j+m}^{[1]} = e_{j+m, i+m}^{[H_m]} = e_{i,j}^{[H_m]}$, and moreover, we can randomly

choose a value of edge feature for $e_{1,m}^{[1]} = e_{m,1}^{[1]} = e_{1+m,2m}^{[1]} = e_{2m,1+m}^{[1]}$. For $G^{[2]}$, let $E^{[2]} = E_{double} \cup \{(1, 2m), (2m, 1), (m, 1+m), (1+m, 2m)\}; \forall i \leq m, x_i^{[2]} = x_{i+m}^{[2]} = x_i^{[H_m]}; \forall (i, j) \in E^{[H_m]}, e_{i,j}^{[1]} = e_{j,i}^{[1]} = e_{i+m,j+m}^{[1]} = e_{j+m,i+m}^{[1]} = e_{i,j}^{[H_m]}$, and moreover, set $e_{1,2m}^{[2]} = e_{2m,1}^{[2]} = e_{m,1+m}^{[2]} = e_{1+m,m}^{[2]} = e_{1,m}^{[1]}$. In words, both $G^{[1]}$ and $G^{[2]}$ are constructed based on two copies of H_m , and the difference is that, $G^{[1]}$ adds the edges $\{(1, m), (m, 1), (1+m, 2m), (2m, 1+m)\}$, whereas $G^{[2]}$ adds the edges $\{(1, 2m), (2m, 1), (m, 1+m), (1+m, m)\}$, all with the same edge feature. For the case $k = 3, m = 8, T = 1$, for example, the constructed graphs are illustrated in Figure 4.

Can $G^{[1]}$ and $G^{[2]}$ be distinguished by k -WL? Let $\mathbf{c}_k^{(t)}, \mathbf{c}'_k^{(t)}$ be the coloring functions of k -tuples for $G^{[1]}$ and $G^{[2]}$, respectively, obtained after running k -WL on the two graphs simultaneously for t iterations. To show that the answer is negative, we want to prove that

$$\{\mathbf{c}_k^{(T)}(s) : s \in [2m]^k\} = \{\mathbf{c}'_k^{(T)}(s) : s \in [2m]^k\} \quad (15)$$

To show this, it is sufficient to find a permutation $\eta : [2m]^k \rightarrow [2m]^k$ such that $\forall k$ -tuple $s \in [2m]^k, \mathbf{c}_k^{(T)}(s) = \mathbf{c}'_k^{(T)}(\eta(s))$. Before defining such an η , we need the following lemma.

Lemma 21. *Let p be a positive integer. If $m \geq (k+1)p$, then $\forall s \in [2m]^k, \exists i \in [m]$ such that $\{i, i+1, \dots, i+p-1\} \cap \{\text{MOD}_m(j) : j \in s\} = \emptyset$.*

Proof of Lemma 21: We can use a simple counting argument to show this. For $u \in [k+1]$, define $A_u = \{up, up+1, \dots, (u+1)p-1\} \cup \{up+m, up+1+m, \dots, (u+1)p-1+m\}$. Then $|A_u| = 2p$, $A_u \cap A_{u'} = \emptyset$ if $u \neq u'$, and

$$[2m] \supseteq \bigcup_{u \in [k+1]} A_u, \quad (16)$$

since $m \geq (k+1)p$. Suppose that the claim is not true, then each A_i contains at least one node in s , and therefore

$$s \supseteq (s \cap [2m]) \supseteq \bigcup_{u \in [k+1]} (s \cap A_u),$$

which contains at least $k+1$ nodes, which is contradictory. \square

With this lemma, we see that $\forall s \in [2m]^k, \exists i \in [m]$ such that $\forall j \in s, \text{MOD}_m(j)$ either $< i$ or $\geq i + 2^{T+1} - 1$. Thus, we can first define the mapping $\chi : [2m]^k \rightarrow [m]$ from a k -tuple s to the smallest such node index $i \in [m]$. Next, $\forall i \in [m]$, we define a mapping τ_i from $[2m]$ to $[2m]$ as

$$\tau_i(j) = \begin{cases} j, & \text{if } \text{MOD}_m(j) \leq i \\ \text{MOD}_{2m}(j+m), & \text{otherwise} \end{cases} \quad (17)$$

τ_i is a permutation on $[2m]$. For $\forall i \in [m]$, this allows us to define a mapping ζ_i from $[2m]^k \rightarrow [2m]^k$ as, $\forall s = (i_1, \dots, i_k) \in [2m]^k$,

$$\zeta_i(s) = (\tau_i(i_1), \dots, \tau_i(i_k)). \quad (18)$$

Finally, we define a mapping η from $[2m]^k \rightarrow [2m]^k$ as,

$$\eta(s) = \zeta_{\chi(s)}(s) \quad (19)$$

The maps χ, τ and η are illustrated in Figure 4.

To fulfill the proof, there are two things we need to show about η . First, we want it to be a permutation on $[2m]^k$. To see this, observe that $\chi(s) = \chi(\eta(s))$, and hence $\forall s \in [2m]^k, (\eta \circ \eta)(s) =$

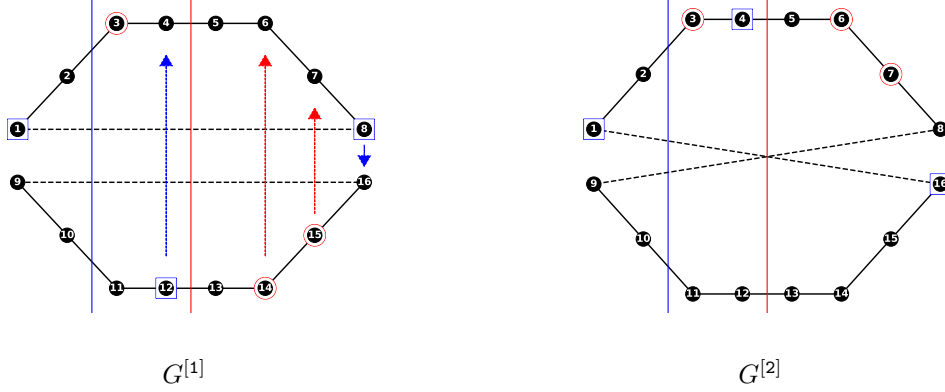


Figure 4: Illustration of the construction in the proof of Theorem 9 in Appendix H. In this particular case, $k = 3$, $m = 8$, $T = 1$. If we consider $s = (1, 12, 8)$ as an example, where the corresponding nodes are marked by blue squares in $G^{[1]}$, there is $\chi(s) = 2$, and thus $\eta(s) = \zeta_2(s) = (1, 4, 16)$, which are marked by blue squares in $G^{[2]}$. Similarly, if we consider $s = (3, 14, 15)$, then $\chi(s) = 4$, and thus $\eta(s) = \zeta_4(s) = (3, 6, 7)$. In both cases, we see that the isomorphism type of s in $G^{[1]}$ equals the isomorphism type of $\eta(s)$ in $G^{[2]}$. In the end, we will show that $\mathbf{c}_k^{(T)}(s) = \mathbf{c}_k^{(T)}(\eta(s))$.

$(\zeta_{\chi(\eta(s))} \circ \zeta_{\chi(s)})(s) = s$, since $\forall i \in [m]$, $\tau_i \circ \tau_i$ is the identity map on $[2m]$.

Second, we need to show that $\forall s \in [2m]^k$, $\mathbf{c}_k^{(T)}(s) = \mathbf{c}_k^{(T)}(\eta(s))$. This will be a consequence of the following lemma.

Lemma 22. *At iteration t , $\forall s \in [2m]^k$, $\forall i$ such that $\forall j \in s$, either $\text{MOD}_m(j) < i$ or $\text{MOD}_m(j) \geq i + 2^t$, there is*

$$\mathbf{c}_k^{(t)}(s) = \mathbf{c}_k^{(t)}(\zeta_i(s)) \quad (20)$$

Remark: This statement allows i to depend on s , as will be the case when we apply this lemma to $\eta(s) = \zeta_{\chi(s)}(s)$, where we set i to be $\chi(s)$.

Proof of Lemma 22: Notation-wise, for any k -tuple, $s = (i_1, \dots, i_k)$, and for $w \in [k]$, use $I_w(s)$ to denote the w th entry of s , i_w .

The lemma can be shown by using induction on t . Before looking at the base case $t = 0$, we will first show the inductive step, which is:

$$\begin{aligned} \forall \bar{T}, \text{ suppose the lemma holds for all } t \leq \bar{T} - 1, \\ \text{ then it also holds for } t = \bar{T}. \end{aligned} \quad (21)$$

Inductive step:

Fix a \bar{T} and suppose the lemma holds for all $t \leq \bar{T} - 1$. Under the condition that $\forall j \in s$, either $\text{MOD}_m(j) < i$ or $\text{MOD}_m(j) \geq i + 2^{\bar{T}}$, to show $\mathbf{c}_k^{(\bar{T})}(s) = \mathbf{c}_k^{(\bar{T})}(\zeta_i(s))$, we need two things to hold:

1. $\mathbf{c}_k^{(\bar{T}-1)}(s) = \mathbf{c}_k^{(\bar{T}-1)}(\zeta_i(s))$
2. $\forall w \in [k]$, $\{\mathbf{c}_k^{(\bar{T}-1)}(\tilde{s}) : \tilde{s} \in N_w(s)\} = \{\mathbf{c}_k^{(\bar{T}-1)}(\tilde{s}) : \tilde{s} \in N_w(\zeta_i(s))\}$

The first condition is a consequence of the inductive hypothesis, as $i + 2^{\bar{T}} > i + 2^{(\bar{T}-1)}$. For the second condition, it is sufficient to find for all $w \in [k]$, a bijective mapping ξ from $N_w(s)$ to $N_w(\zeta_i(s))$

such that $\forall \tilde{s} \in N_w(s)$, $\mathbf{c}_k^{(\bar{T}-1)}(\tilde{s}) = \mathbf{c}'_k^{(\bar{T}-1)}(\xi(\tilde{s}))$.

We then define $\beta(i, \tilde{s}) =$

$$\begin{cases} \text{MOD}_m(\mathbf{I}_w(\tilde{s})) + 1, & \text{if } i \leq \text{MOD}_m(\mathbf{I}_w(\tilde{s})) < i + 2^{\bar{T}-1} \\ i, & \text{otherwise} \end{cases} \quad (22)$$

Now, consider any $\tilde{s} \in N_w(s)$. Note that \tilde{s} and s differ only in the w th entry of the k -tuple.

- If $i \leq \text{MOD}_m(\mathbf{I}_w(\tilde{s})) < i + 2^{\bar{T}-1}$, then $\forall j \in \tilde{s}$,
 - either $j \in s$, in which case either $\text{MOD}_m(j) < i < \text{MOD}_m(\mathbf{I}_w(\tilde{s})) + 1 = \beta(i, \tilde{s})$ or $\text{MOD}_m(j) \geq i + 2^{\bar{T}} \geq \text{MOD}_m(\mathbf{I}_w(\tilde{s})) + 1 + 2^{\bar{T}-1} = \beta(i, \tilde{s}) + 2^{\bar{T}-1}$,
 - or $j = \mathbf{I}_w(\tilde{s})$, in which case $\text{MOD}_m(j) < \text{MOD}_m(\mathbf{I}_w(\tilde{s})) + 1 = \beta(i, \tilde{s})$.
- If $\text{MOD}_m(\mathbf{I}_w(\tilde{s})) < i$ or $\text{MOD}_m(\mathbf{I}_w(\tilde{s})) \geq i + 2^{\bar{T}-1}$, then $\forall j \in \tilde{s}$,
 - either $j \in s$, in which case either $\text{MOD}_m(j) < i = \beta(i, \tilde{s})$ or $\text{MOD}_m(j) \geq i + 2^{\bar{T}} \geq \beta(i, \tilde{s}) + 2^{\bar{T}-1}$,
 - or $j = \mathbf{I}_w(\tilde{s})$, in which case either $\text{MOD}_m(j) < i = \beta(i, \tilde{s})$ or $\text{MOD}_m(j) \geq i + 2^{\bar{T}-1} \geq \beta(i, \tilde{s}) + 2^{\bar{T}-1}$.

Thus, in all cases, there is $\forall j \in \tilde{s}$, either $\text{MOD}_m(j) < \beta(i, \tilde{s})$, or $\text{MOD}_m(j) \geq i + 2^{\bar{T}-1}$. Hence, by the inductive hypothesis, we have $\mathbf{c}_k^{(\bar{T}-1)}(\tilde{s}) = \mathbf{c}'_k^{(\bar{T}-1)}(\zeta_{\beta(i, \tilde{s})}(\tilde{s}))$. This inspires us to define, for $\forall w \in [k]$, $\forall \tilde{s} \in N_w(s)$,

$$\xi(\tilde{s}) = \zeta_{\beta(i, \tilde{s})}(\tilde{s}) \quad (23)$$

Additionally, we still need to prove that, firstly, ξ maps $N_w(s)$ to $N_w(\zeta_i(s))$, and secondly, ξ is a bijection. For the first statement, note that $\forall \tilde{s} \in N_w(s)$, $\zeta_{\beta(i, \tilde{s})}(s) = \zeta_i(s)$ because s contains no entry between i and $\beta(i, \tilde{s})$, with the latter being less than $i + 2^{\bar{T}}$. Hence, if $\tilde{s} \in N_w(s)$, then $\forall w' \in [k]$ with $w' \neq w$, there is $\mathbf{I}_{w'}(\tilde{s}) = \mathbf{I}_{w'}(s)$, and therefore $\mathbf{I}_{w'}(\xi(\tilde{s})) = \mathbf{I}_{w'}(\zeta_{\beta(i, \tilde{s})}(\tilde{s})) = \tau_{\beta(i, \tilde{s})}(\mathbf{I}_{w'}(\tilde{s})) = \tau_{\beta(i, \tilde{s})}(\mathbf{I}_{w'}(s)) = \mathbf{I}_{w'}(\zeta_{\beta(i, \tilde{s})}(s)) = \mathbf{I}_{w'}(\zeta_i(s))$, which ultimately implies that $\xi(\tilde{s}) \in N_w(\zeta_i(s))$.

For the second statement, note that since $\mathbf{I}_w(\xi(\tilde{s})) = \tau_{\beta(i, \tilde{s})}(\mathbf{I}_w(\tilde{s}))$ (by the definition of ζ), there is $\text{MOD}_m(\mathbf{I}_w(\xi(\tilde{s}))) = \text{MOD}_m(\tau_{\beta(i, \tilde{s})}(\mathbf{I}_w(\tilde{s}))) = \text{MOD}_m(\mathbf{I}_w(\tilde{s}))$, and therefore $\beta(i, \xi(\tilde{s})) = \beta(i, \tilde{s})$. Thus, we know that $(\xi \circ \xi)(\tilde{s}) = (\zeta_{\beta(i, \xi(\tilde{s}))} \circ \zeta_{\beta(i, \tilde{s})})(\tilde{s}) = (\zeta_{\beta(i, \tilde{s})} \circ \zeta_{\beta(i, \tilde{s})})(\tilde{s}) = \tilde{s}$. This implies that ξ is a bijection from $N_w(s)$ to $N_w(\zeta_i(s))$.

This concludes the proof of the inductive step.

Base case:

We need to show that

$$\begin{aligned} \forall s \in [2m]^k, \forall i^* \text{ such that } \forall j \in s, \text{ either } \text{MOD}_m(j) < i^* \\ \text{or } \text{MOD}_m(j) \geq i^* + 1, \text{ there is } \mathbf{c}_k^{(0)}(s) = \mathbf{c}'_k^{(0)}(\zeta_{i^*}(s)) \end{aligned} \quad (24)$$

Due to the way in which the colorings of the k -tuples are initialized in k -WL, the statement above is equivalent to showing that s in $G^{[1]}$ and $\zeta_{i^*}(s)$ in $G^{[2]}$ have the same isomorphism type, for which we need the following to hold.

Lemma 23. *Say $s = (i_1, \dots, i_k)$, in which case $\zeta_{i^*}(s) = (\tau_{i^*}(i_1), \dots, \tau_{i^*}(i_k))$. Then*

1. $\forall i_\alpha, i_\beta \in s, i_\alpha = i_\beta \Leftrightarrow \tau_{i^*}(i_\alpha) = \tau_{i^*}(i_\beta)$

2. $\forall i_\alpha \in s, x_{i_\alpha}^{[1]} = x_{\tau_{i^*}^{[2]}(i_\alpha)}^{[2]}$
3. $\forall i_\alpha, i_\beta \in s, (i_\alpha, i_\beta) \in E^{[1]} \Leftrightarrow (\tau_{i^*}^{[2]}(i_\alpha), \tau_{i^*}^{[2]}(i_\beta)) \in E^{[2]}$, and moreover, if either is true, $e_{i_\alpha, i_\beta}^{[1]} = e_{\tau_{i^*}^{[2]}(i_\alpha), \tau_{i^*}^{[2]}(i_\beta)}^{[2]}$

Proof of Lemma 23:

1. This is true since τ_{i^*} is a permutation on $[2m]$.
2. This is true because by the construction of the two graphs, $\forall i \in [2m], x_i^{[1]} = x_i^{[2]}$, and moreover $x_i^{[1]} = x_{i+m}^{[1]}$ if $i \leq m$.
3. Define $S = \{(1, m), (m, 1), (1+m, 2m), (2m, 1+m), (1, 2m), (2m, 1), (m, 1+m), (1+m, 2m)\}$, which is the set of ‘‘special’’ pairs of nodes in which $G^{[1]}$ and $G^{[2]}$ differ. Note that $\forall (i_\alpha, i_\beta) \in [2m]^2, (i_\alpha, i_\beta) \in S$ if and only if the sets $\{\text{MOD}_m(i_\alpha), \text{MOD}_m(i_\beta)\} = \{1, m\}$.
By the assumption on i^* in (24), we know that $i_\alpha, i_\beta \notin \{i^*, i^* + m\}$. Now we look at 16 different cases separately, which comes from 4 possibilities for each of i_α and i_β : i_α (or i_β) belonging to $\{1, \dots, i^* - 1\}, \{i^* + 1, \dots, m\}, \{1 + m, \dots, i^* - 1 + m\}$, or $\{i^* + 1 + m, \dots, 2m\}$

Case 1 $1 \leq i_\alpha, i_\beta < i^*$

Then $\tau_{i^*}(i_\alpha) = i_\alpha, \tau_{i^*}(i_\beta) = i_\beta$. In addition, as $\text{MOD}_m(i_\alpha), \text{MOD}_m(i_\beta) \neq m$, there is $(i_\alpha, i_\beta) \notin S$. Thus, if $(i_\alpha, i_\beta) \in E^{[1]}$, then $(i_\alpha, i_\beta) \in E_{\text{double}} \subset E^{[2]}$, and moreover, $e_{i_\alpha, i_\beta}^{[1]} = e_{i_\alpha, i_\beta}^{[H_m]} = e_{i_\alpha, i_\beta}^{[2]} = e_{\tau_{i^*}^{[2]}(i_\alpha), \tau_{i^*}^{[2]}(i_\beta)}^{[2]}$. Same for the other direction.

Case 2 $1 + m \leq i_\alpha, i_\beta < i^* + m$

Similar to case 1.

Case 3 $i^* + 1 \leq i_\alpha, i_\beta \leq m$

Then $\tau_{i^*}(i_\alpha) = i_\alpha + m, \tau_{i^*}(i_\beta) = i_\beta + m$. In addition, as $\text{MOD}_m(i_\alpha), \text{MOD}_m(i_\beta) \neq 1$, there is $(i_\alpha, i_\beta) \notin S$. Thus, if $(i_\alpha, i_\beta) \in E^{[1]}$, then $(i_\alpha, i_\beta) \in E_{\text{double}}$, and hence $(i_\alpha + m, i_\beta + m) \in E_{\text{double}} \subset E^{[2]}$, and moreover, $e_{i_\alpha, i_\beta}^{[1]} = e_{i_\alpha, i_\beta}^{[H_m]} = e_{i_\alpha + m, i_\beta + m}^{[2]} = e_{\tau_{i^*}^{[2]}(i_\alpha), \tau_{i^*}^{[2]}(i_\beta)}^{[2]}$.

Case 4 $i^* + 1 + m \leq i_\alpha, i_\beta \leq 2m$

Similar to case 3.

Case 5 $1 \leq i_\alpha < i^*, i^* + 1 \leq i_\beta \leq m$

If $i_\alpha \neq 1$ or $i_\beta \neq m$, then since H_m is a path and $i_\alpha < i^* \leq i_\beta - 1$, $(i_\alpha, i_\beta) \notin E^{[1]}$ or $E^{[2]}$. Now we consider the case where $i_\alpha = 1, i_\beta = m$. As $1 \leq i^* < m$, by the definition of τ , there is $\tau_{i^*}(1) = 1$, and $\tau_{i^*}(m) = 2m$. Note that both $(1, m) \in E^{[1]}$ and $(1, 2m) \in E^{[2]}$ are true, and moreover, $e_{1, m}^{[1]} = e_{1, 2m}^{[2]}$.

Case 6 $1 \leq i_\beta < i^*, i^* + 1 \leq i_\alpha \leq m$

Similar to case 5.

Case 7 $1 + m \leq i_\alpha < i^* + m, i^* + 1 + m \leq i_\beta \leq 2m$

Similar to case 5.

Case 8 $1 + m \leq i_\beta < i^* + m, i^* + 1 + m \leq i_\alpha \leq 2m$

Similar to case 5.

Case 9 $1 \leq i_\alpha < i^*$ and $1 + m \leq i_\beta < i^* + m$

Then $\tau_s(i_\alpha) = i_\alpha, \tau_s(i_\beta) = i_\beta$, and $(i_\alpha, i_\beta) \notin E^{[1]}$ or $E^{[2]}$.

Case 10 $1 \leq i_\beta < i^*$ and $1 + m \leq i_\alpha < i^* + m$

Similar to case 9.

Case 11 $i^* + 1 \leq i_\alpha < m$ and $i^* + 1 + m \leq i_\beta \leq 2m$

$(i_\alpha, i_\beta) \notin E^{[1]}$. $\tau_s(i_\alpha) = i_\alpha + m, \tau_s(i_\beta) = i_\beta - m$. Hence $(\tau_s(i_\alpha), \tau_s(i_\beta)) \notin E^{[2]}$ either.

Case 12 $i^* + 1 \leq i_\beta \leq m$ and $i^* + 1 + m \leq i_\alpha \leq 2m$

Similar to case 11.

Case 13 $1 \leq i_\alpha < i^*$ and $i^* + 1 + m \leq i_\beta \leq 2m$

$(i_\alpha, i_\beta) \notin E^{[1]}$ obviously. We also have $\tau_s(i_\alpha) = i_\alpha \in [1, i^*]$, $\tau_s(i_\beta) = i_\beta - 1 \in [i^* + 1, m]$, and hence $(\tau_s(i_\alpha), \tau_s(i_\beta)) \notin E^{[2]}$.

Case 14 $1 \leq i_\beta < i^*$ and $i^* + 1 + m \leq i_\alpha \leq 2m$

Similar to case 13.

Case 15 $1 + m \leq i_\alpha < i^* + m$ and $i^* + 1 \leq i_\beta \leq m$

Similar to case 13.

Case 16 $1 + m \leq i_\beta < i^* + m$ and $i^* + 1 \leq i_\alpha \leq m$

Similar to case 13.

This concludes the proof of Lemma 23. □

Lemma 23 completes the proof of the base case, and hence the induction argument for Lemma 22. □

$\forall s \in [2m]^k$, since $\eta(s) = \zeta_{\chi(s)}(s)$, and $\chi(s)$ satisfies $\forall j \in s$, either $\text{MOD}_m(j) < i$ or $\text{MOD}_m(j) \geq i + 2^T$, Lemma 22 implies that at iteration T , we have $\mathbf{c}_k^{(T)}(s) = \mathbf{c}'_k^{(T)}(\zeta_{\chi(s)}(s)) = \mathbf{c}'_k^{(T)}(\eta(s))$. Since we have shown that η is a permutation on $[2m]^k$, this let's us conclude that

$$\{\mathbf{c}_k^{(T)}(s) : s \in [2m]^k\} = \{\mathbf{c}'_k^{(T)}(s) : s \in [2m]^k\}, \quad (25)$$

and therefore k -WL cannot distinguish between the two graphs in T iterations. □

I Proof of Theorem 11 (2-IGNs are no more powerful than 2-WL)

Note that a 2-IGN takes as input a third-order tensor, $\mathbf{B}^{(0)}$, defined for a given graph $G = (V = [n], E, x, e)$ in the following way. Supposing without loss of generality that the node and edge features both have dimension d , we have $\mathbf{B}^{(0)} \in \mathbb{R}^{n \times n \times (d+1)}$, such that: $\forall i \in [n]$, $\mathbf{B}_{i,i,2:(d+1)}^{(0)} = x_i$; $\forall i, j \in [n]$ with $i \neq j$, $\mathbf{B}_{i,j,1}^{(0)} = A_{i,j}$ and $\mathbf{B}_{i,j,2:(d+1)}^{(0)} = e_{i,j}$. If we use $\mathbf{B}^{(t)}$ to denote the output of the t th layer of the 2-IGN, then they are obtained iteratively by

$$\mathbf{B}^{(t+1)} = \sigma(L^{(t)}(\mathbf{B}^{(t)})) \quad (26)$$

Proof. For simplicity of notations, we assume $d_t = 1$ in every layer of a 2-IGN. The general case can be proved by adding more subscripts. For 2-WL, we use the definition in section 3.1 except for omitting the subscript k in $\mathbf{c}_k^{(t)}$.

To start, it is straightforward to show (and we will prove it at the end) that the theorem can be deduced from the following lemma:

Lemma 24. *Say $G^{[1]}$ and $G^{[2]}$ cannot be distinguished by the 2-WL. Then $\forall t \in \mathbb{N}$, it holds that*

$$\forall s, s' \in V^2, \text{ if } \mathbf{c}^{(t)}(s) = \mathbf{c}'^{(t)}(s'), \text{ then } \mathbf{B}_s^{(t)} = \mathbf{B}'_{s'}^{(t)} \quad (27)$$

This lemma can be shown by induction. To see this, first note that the lemma is equivalent to the statement that

$$\forall T \in \mathbb{N}, \forall t \leq T, (27) \text{ holds.}$$

This allows us to carry out an induction in $T \in \mathbb{N}$. For the base case $t = T = 0$, this is true because $\mathbf{c}^{(0)}$ and $\mathbf{c}'^{(0)}$ in WL and $\mathbf{B}^{(0)}$ and $\mathbf{B}'^{(0)}$ in 2-IGN are both initialized in the same way according to the subgraph isomorphism. To be precise, $\mathbf{c}^{(0)}(s) = \mathbf{c}'^{(0)}(s')$ if and only if the subgraph in $G^{[1]}$ induced by the pair of nodes s is isomorphic to the subgraph in $G^{[2]}$ induced by the pair of nodes s' , which is also true if and only if $\mathbf{B}_s^{(0)} = \mathbf{B}_{s'}^{(0)}$.

Next, to show that the induction step holds, we need to prove the following statement:

$$\begin{aligned} \forall T \in \mathbb{N}, \text{ if } \forall t \leq T-1, (27) \text{ holds,} \\ \text{ then } (27) \text{ also holds for } t = T. \end{aligned}$$

To prove the consequent, we assume that for some $s, s' \in V^2$, there is $\mathbf{c}^{(T)}(s) = \mathbf{c}'^{(T)}(s')$, and then attempt to show that $\mathbf{B}_s^{(T)} = \mathbf{B}_{s'}^{(T)}$. By the update rules of k -WL, the statement $\mathbf{c}^{(T)}(s) = \mathbf{c}'^{(T)}(s')$ implies that

$$\begin{cases} \mathbf{c}^{(T-1)}(s) = \mathbf{c}'^{(T-1)}(s') \\ \{\mathbf{c}^{(T-1)}(\tilde{s}) : \tilde{s} \in N_1(s)\} = \{\mathbf{c}'^{(T-1)}(\tilde{s}) : \tilde{s} \in N_1(s')\} \\ \{\mathbf{c}^{(T-1)}(\tilde{s}) : \tilde{s} \in N_2(s)\} = \{\mathbf{c}'^{(T-1)}(\tilde{s}) : \tilde{s} \in N_2(s')\} \end{cases} \quad (28)$$

Case 1: $s = (i, j) \in V^2$ **with** $i \neq j$

Let's first consider the case where $s = (i, j) \in V^2$ with $i \neq j$. In this case, we can also write $s' = (i', j') \in V^2$ with $i' \neq j'$, thanks to Lemma 18. Then, note that V^2 can be written as the union of 9 disjoint sets that are defined depending on s :

$$V^2 = \bigcup_{w=1}^9 A_{s,w},$$

where we define $A_{s,1} = \{(i, j)\}$, $A_{s,2} = \{(i, i)\}$, $A_{s,3} = \{(j, j)\}$, $A_{s,4} = \{(i, k) : k \neq i \text{ or } j\}$, $A_{s,5} = \{(k, i) : k \neq i \text{ or } j\}$, $A_{s,6} = \{(j, k) : k \neq i \text{ or } j\}$, $A_{s,7} = \{(k, j) : k \neq i \text{ or } j\}$, $A_{s,8} = \{(k, l) : k \neq l \text{ and } \{k, l\} \cap \{i, j\} = \emptyset\}$, and $A_{s,9} = \{(k, k) : k \notin \{i, j\}\}$. In this way, we partition V^2 into 9 different subsets, each of which consisting of pairs (k, l) that yield a particular equivalence class of the 4-tuple (i, j, k, l) . Similarly, we can define $A_{s',w}$ for $w \in [9]$, which will also give us

$$V^2 = \bigcup_{w=1}^9 A_{s',w}$$

Moreover, note that

$$\begin{aligned} N_1(s) &= \bigcup_{w=1,3,7} A_{s,w} \\ N_2(s) &= \bigcup_{w=1,2,4} A_{s,w} \\ N_1(s') &= \bigcup_{w=1,3,7} A_{s',w} \\ N_2(s') &= \bigcup_{w=1,2,4} A_{s',w} \end{aligned}$$

Before proceeding, we make the following definition to simplify notations:

$$\mathbf{c}_{s,w} = \{\mathbf{c}^{(T-1)}(\tilde{s}) : \tilde{s} \in A_{s,w}\}$$

$$\mathfrak{C}'_{s',w} = \{\mathfrak{c}'^{(T-1)}(\tilde{s}) : \tilde{s} \in A_{s',w}\}$$

This allows us to rewrite (28) as

$$\mathfrak{C}_{s,1} = \mathfrak{C}'_{s',1} \quad (29)$$

$$\bigcup_{w=1,3,7} \mathfrak{C}_{s,w} = \bigcup_{w=1,3,7} \mathfrak{C}'_{s',w} \quad (30)$$

$$\bigcup_{w=1,2,4} \mathfrak{C}_{s,w} = \bigcup_{w=1,2,4} \mathfrak{C}'_{s',w} \quad (31)$$

Combining (29) and (30), we obtain

$$\bigcup_{w=3,7} \mathfrak{C}_{s,w} = \bigcup_{w=3,7} \mathfrak{C}'_{s',w} \quad (32)$$

Combining (29) and (31), we obtain

$$\bigcup_{w=2,4} \mathfrak{C}_{s,w} = \bigcup_{w=2,4} \mathfrak{C}'_{s',w} \quad (33)$$

Note that V^2 can also be partitioned into two disjoint subsets:

$$V^2 = \left(\bigcup_{w=1,4,5,6,7,8} A_{s,w} \right) \cap \left(\bigcup_{w=2,3,9} A_{s,w} \right),$$

where the first subset represent the edges: $\{(i,j) \in V^2 : i \neq j\}$ and the second subset represent the nodes: $\{(i,i) : i \in V\}$. Similarly,

$$V^2 = \left(\bigcup_{w=1,4,5,6,7,8} A_{s',w} \right) \cap \left(\bigcup_{w=2,3,9} A_{s',w} \right),$$

As shown in Lemma 18, pairs of nodes that represent edges cannot share the same color with pairs of nodes the represent nodes in any iteration of 2-WL. Thus, we have

$$\left(\bigcup_{w=1,4,5,6,7,8} \mathfrak{C}_{s,w} \right) \cap \left(\bigcup_{w=2,3,9} \mathfrak{C}'_{s',w} \right) = \emptyset \quad (34)$$

$$\left(\bigcup_{w=1,4,5,6,7,8} \mathfrak{C}'_{s',w} \right) \cap \left(\bigcup_{w=2,3,9} \mathfrak{C}_{s,w} \right) = \emptyset \quad (35)$$

Combining (32) and (34) or (35), we get

$$\mathfrak{C}_{s,3} = \mathfrak{C}'_{s',3} \quad (36)$$

$$\mathfrak{C}_{s,7} = \mathfrak{C}'_{s',7} \quad (37)$$

Combining (33) and (34) or (35), we get

$$\mathfrak{C}_{s,2} = \mathfrak{C}'_{s',2} \quad (38)$$

$$\mathfrak{C}_{s,4} = \mathfrak{C}'_{s',4} \quad (39)$$

Thanks to symmetry between (i,j) and (j,i) , as we work with undirected graphs, there is

$$\mathfrak{C}_{s,5} = \mathfrak{C}_{s,4} = \mathfrak{C}'_{s',4} = \mathfrak{C}'_{s',5} \quad (40)$$

$$\mathfrak{C}_{s,6} = \mathfrak{C}_{s,7} = \mathfrak{C}'_{s',7} = \mathfrak{C}'_{s',6} \quad (41)$$

In addition, since we assume that $G^{[1]}$ and $G^{[2]}$ cannot be distinguished by 2-WL, there has to be

$$\bigcup_{w=1}^9 \mathfrak{C}_{s,w} = \bigcup_{w=1}^9 \mathfrak{C}'_{s',w}$$

Combining this with (34) or (35), we get

$$\bigcup_{w=1,4,5,6,7,8} \mathfrak{C}_{s,w} = \bigcup_{w=1,4,5,6,7,8} \mathfrak{C}'_{s',w} \quad (42)$$

$$\bigcup_{w=2,3,9} \mathfrak{C}_{s,w} = \bigcup_{w=2,3,9} \mathfrak{C}'_{s',w} \quad (43)$$

Combining (42) with (29), (39), (40), (41), (37), we get

$$\mathfrak{C}_{s,8} = \mathfrak{C}'_{s',8} \quad (44)$$

Combining (43) with (38) and (36), we get

$$\mathfrak{C}_{s,9} = \mathfrak{C}'_{s',9} \quad (45)$$

Hence, in conclusion, we have that $\forall w \in [9]$,

$$\mathfrak{C}_{s,w} = \mathfrak{C}'_{s',w} \quad (46)$$

By the inductive hypothesis, this implies that $\forall w \in [9]$,

$$\{\mathbf{B}_{\tilde{s}}^{(T-1)} : \tilde{s} \in A_{s,w}\} = \{\mathbf{B}'_{\tilde{s}}^{(T-1)} : \tilde{s} \in A_{s',w}\} \quad (47)$$

Let us show how (47) may be leveraged. First, to prove that $\mathbf{B}_s^{(T)} = \mathbf{B}'_{s'}^{(T)}$, recall that

$$\begin{aligned} \mathbf{B}^{(T)} &= \sigma(L^{(T)}(\mathbf{B}^{(T-1)})) \\ \mathbf{B}'^{(T)} &= \sigma(L^{(T)}(\mathbf{B}'^{(T-1)})) \end{aligned} \quad (48)$$

Therefore, it is sufficient to show that for all linear equivariant layer L , we have

$$L(\mathbf{B}^{(T-1)})_{i,j} = L(\mathbf{B}'^{(T-1)})_{i',j'} \quad (49)$$

Also, recall that

$$\begin{aligned} L(\mathbf{B}^{(T-1)})_{i,j} &= \sum_{(k,l) \in V^2} T_{i,j,k,l} \mathbf{B}_{k,l} + Y_{i,j} \\ L(\mathbf{B}'^{(T-1)})_{i',j'} &= \sum_{(k',l') \in V^2} T_{i',j',k',l'} \mathbf{B}'_{k',l'} + Y_{i',j'} \end{aligned} \quad (50)$$

By the definition of the $A_{s,w}$'s and $A_{s',w}$'s, there is $\forall w \in [9], \forall (k,l) \in A_{s,w}, \forall (k',l') \in A_{s',w}$, we have the 4-tuples $(i,j,k,l) \sim (i',j',k',l')$, i.e., \exists a permutation π on V such that $(i,j,k,l) = (\pi(i'), \pi(j'), \pi(k'), \pi(l'))$, which implies that $T_{i,j,k,l} = T_{i',j',k',l'}$. Therefore, together with (47), we have the following:

$$\begin{aligned} L(\mathbf{B}^{(T-1)})_{i,j} &= \sum_{(k,l) \in V^2} T_{i,j,k,l} \mathbf{B}_{k,l} + Y_{i,j} \\ &= \sum_{w=1}^9 \sum_{(k,l) \in A_{s,w}} T_{i,j,k,l} \mathbf{B}_{k,l} + Y_{i,j} \\ &= \sum_{w=1}^9 \sum_{(k',l') \in A_{s',w}} T_{i',j',k',l'} \mathbf{B}'_{k',l'} + Y_{i',j'} \\ &= L(\mathbf{B}'^{(T-1)})_{i',j'} \end{aligned} \quad (51)$$

and hence $\mathbf{B}_{i,j}^{(T)} = \mathbf{B}_{i',j'}^{(T)}$, which concludes the proof for the case that $s = (i, j)$ for $i \neq j$.

Case 2: $s = (i, i) \in V^2$

Next, consider the case $s = (i, i) \in V^2$. In this case, $s' = (i', i')$ for some $i' \in V$. This time, we write V^2 as the union of 5 disjoint sets that depend on s (or s'):

$$V^2 = \bigcup_{w=1}^5 A_{s,w},$$

where we define $A_{s,1} = \{(i, i)\}$, $A_{s,2} = \{(i, j) : j \neq i\}$, $A_{s,3} = \{(j, i) : j \neq i\}$, $A_{s,4} = \{(j, k) : j, k \neq i \text{ and } j \neq k\}$, and $A_{s,5} = \{(j, j) : j \neq i\}$. Similar for s' . We can also define $\mathfrak{C}_{s,w}$ and $\mathfrak{C}'_{s',w}$ as above. Note that

$$\begin{aligned} N_1(s) &= \bigcup_{w=1,3} A_{s,w} \\ N_2(s) &= \bigcup_{w=1,2} A_{s,w} \\ N_1(s') &= \bigcup_{w=1,3} A_{s',w} \\ N_2(s') &= \bigcup_{w=1,2} A_{s',w} \end{aligned}$$

Hence, we can rewrite (28) as

$$\mathfrak{C}_{s,1} = \mathfrak{C}'_{s',1} \tag{52}$$

$$\bigcup_{w=1,3} \mathfrak{C}_{s,w} = \bigcup_{w=1,3} \mathfrak{C}'_{s',w} \tag{53}$$

$$\bigcup_{w=1,2} \mathfrak{C}_{s,w} = \bigcup_{w=1,2} \mathfrak{C}'_{s',w} \tag{54}$$

Combining (52) with (53), we get

$$\mathfrak{C}_{s,3} = \mathfrak{C}'_{s',3} \tag{55}$$

Combining (52) with (54), we get

$$\mathfrak{C}_{s,2} = \mathfrak{C}'_{s',2} \tag{56}$$

Moreover, since we can decompose V^2 as

$$\begin{aligned} V^2 &= \left(\bigcup_{w=1,5} A_{s,w} \right) \cup \left(\bigcup_{w=2,3,4} A_{s,w} \right) \\ &= \left(\bigcup_{w=1,5} A_{s',w} \right) \cup \left(\bigcup_{w=2,3,4} A_{s',w} \right) \end{aligned}$$

with $\bigcup_{w=1,5} A_{s,w} = \bigcup_{w=1,5} A_{s',w}$ representing the nodes and $\bigcup_{w=2,3,4} A_{s,w} = \bigcup_{w=2,3,4} A_{s',w}$ representing the edges, we have

$$\left(\bigcup_{w=1,5} \mathfrak{C}_{s,w} \right) \cap \left(\bigcup_{w=2,3,4} \mathfrak{C}'_{s',w} \right) = \emptyset \tag{57}$$

$$\left(\bigcup_{w=1,5} \mathfrak{C}'_{s',w} \right) \cap \left(\bigcup_{w=2,3,4} \mathfrak{C}_{s,w} \right) = \emptyset \tag{58}$$

Since $G^{[1]}$ and $G^{[2]}$ cannot be distinguished by 2-WL, there is

$$\bigcup_{w=1}^5 \mathfrak{C}_{s,w} = \bigcup_{w=1}^5 \mathfrak{C}'_{s',w}$$

Therefore, combining this with (57) or (58), we obtain

$$\bigcup_{w=1,5} \mathfrak{C}_{s,w} = \bigcup_{w=1,5} \mathfrak{C}'_{s',w} \quad (59)$$

$$\bigcup_{w=2,3,4} \mathfrak{C}_{s,w} = \bigcup_{w=2,3,4} \mathfrak{C}'_{s',w} \quad (60)$$

Combining (59) with (52), we get

$$\mathfrak{C}_{s,5} = \mathfrak{C}'_{s',5} \quad (61)$$

Combining (60) with (56) and (55), we get

$$\mathfrak{C}_{s,4} = \mathfrak{C}'_{s',4} \quad (62)$$

Hence, in conclusion, we have that $\forall w \in [5]$,

$$\mathfrak{C}_{s,w} = \mathfrak{C}'_{s',w} \quad (63)$$

By the inductive hypothesis, this implies that $\forall w \in [5]$,

$$\{\mathbf{B}_{\tilde{s}}^{(T-1)} : \tilde{s} \in A_{s,w}\} = \{\mathbf{B}'_{\tilde{s}}^{(T-1)} : \tilde{s} \in A_{s',w}\} \quad (64)$$

Thus,

$$\begin{aligned} L(\mathbf{B}^{(T-1)})_{i,i} &= \sum_{(k,l) \in V^2} T_{i,i,k,l} \mathbf{B}_{k,l} + Y_{i,i} \\ &= \sum_{w=1}^5 \sum_{(k,l) \in A_{s,w}} T_{i,i,k,l} \mathbf{B}_{k,l} + Y_{i,i} \\ &= \sum_{w=1}^5 \sum_{(k',l') \in A_{s',w}} T_{i',i',k',l'} \mathbf{B}'_{k',l'} + Y_{i',i'} \\ &= L(\mathbf{B}'^{(T-1)})_{i',i'} \end{aligned}$$

and hence $\mathbf{B}_{i,j}^{(T)} = \mathbf{B}'_{i',j'}^{(T)}$, which concludes the proof for the case that $s = (i, i)$ for $i \in V$. \square

Now, suppose we are given any 2-IGN with T layers. Since $G^{[1]}$ and $G^{[2]}$ cannot be distinguished by 2-WL, together with Lemma 18, there is

$$\{\mathbf{c}^{(T)}((i, j)) : i, j \in V, i \neq j\} = \{\mathbf{c}'^{(T)}((i', j')) : i', j' \in V, i' \neq j'\}$$

and

$$\{\mathbf{c}^{(T)}((i, i)) : i \in V\} = \{\mathbf{c}'^{(T)}((i', i')) : i' \in V\}$$

Hence, by the lemma, we have

$$\{\mathbf{B}_{(i,j)}^{(T)} : i, j \in V, i \neq j\} = \{\mathbf{B}'_{(i',j')}^{(T)} : i', j' \in V, i' \neq j'\}$$

and

$$\{\mathbf{B}_{(i,i)}^{(T)} : i \in V\} = \{\mathbf{B}'_{(i',i')}^{(T)} : i' \in V\}$$

Then, since the second-last layer h in the 2-IGN can be written as

$$h(\mathbf{B}) = \alpha \sum_{i,j \in V, i \neq j} \mathbf{B}_{i,j} + \beta \sum_{i \in V} \mathbf{B}_{i,i} \quad (65)$$

there is

$$h(\mathbf{B}^{(T)}) = h(\mathbf{B}'^{(T)}) \quad (66)$$

and finally

$$m \circ h(\mathbf{B}^{(T)}) = m \circ h(\mathbf{B}'^{(T)}) \quad (67)$$

which means the 2-IGN yields identical outputs on the two graphs.

J Direct proof of Corollary 13 (2-IGNs are unable to induced-subgraph-count patterns of 3 or more nodes)

Proof. The same counterexample as in the proof of Theorem 3 given in Appendix E applies here, as we are going to show below. Note that we only need to consider the non-clique case, since the set of counterexample graphs for the non-clique case is a superset of the set of counterexample graphs for the clique case.

Let \mathbf{B} be the input tensor corresponding to $G^{[1]}$, and \mathbf{B}' corresponding to $G^{[2]}$. For simplicity, we assume in the proof below that $d_0, \dots, d_T = 1$. The general case can be proved in the same way but with more subscripts. (In particular, for our counterexamples, (71) can be shown to hold for each of the d_0 feature dimensions.)

Define a set $S = \{(1, 2), (2, 1), (1+m, 2+m), (2+m, 1+m), (1, 2+m), (2+m, 1), (1+m, 2), (2, 1+m)\}$, which represents the “special” edges that capture the difference between $G^{[1]}$ and $G^{[2]}$. We aim to show something like this:

$\forall t,$

$$\left\{ \begin{array}{l} \mathbf{B}_{i,j}^{(t)} = \mathbf{B}'_{i,j}^{(t)}, \forall (i, j) \notin S \\ \mathbf{B}_{1,2}^{(t)} = \mathbf{B}'_{1+m,2}^{(t)}, \\ \mathbf{B}_{2,1}^{(t)} = \mathbf{B}'_{2,1+m}^{(t)}, \\ \mathbf{B}_{1+m,2+m}^{(t)} = \mathbf{B}'_{1,2+m}^{(t)} \\ \mathbf{B}_{2+m,1+m}^{(t)} = \mathbf{B}'_{2+m,1}^{(t)} \\ \mathbf{B}_{1,2+m}^{(t)} = \mathbf{B}'_{1+m,2+m}^{(t)}, \\ \mathbf{B}_{2+m,1}^{(t)} = \mathbf{B}'_{2+m,1+m}^{(t)}, \\ \mathbf{B}_{1+m,2}^{(t)} = \mathbf{B}'_{1,2}^{(t)} \\ \mathbf{B}_{2,1+m}^{(t)} = \mathbf{B}'_{2,1}^{(t)} \end{array} \right. \quad (68)$$

If this is true, then it is not hard to show that the 2-IGN returns identical outputs on \mathbf{B} and \mathbf{B}' , which we will leave to the very end. To represent the different cases above compactly, we define a permutation η_1 on $V \times V$ in the following way. First, define the following permutations on V :

$$\kappa_1(i) = \begin{cases} \text{MOD}_{2m}(1+m), & \text{if } i \in \{1, 1+m\} \\ i, & \text{otherwise} \end{cases}$$

Next, define the permutation τ_1 on $V \times V$:

$$\tau_1((i, j)) = (\kappa_1(i), \kappa_1(j))$$

and then η_1 as the restriction of τ_1 on the set $S \subset V \times V$:

$$\eta_1((i, j)) = \begin{cases} \tau_1((i, j)), & \text{if } (i, j) \in S \\ (i, j), & \text{otherwise} \end{cases}$$

Thus, (68) can be rewritten as

$$\forall t, \mathbf{B}_{i,j}^{(t)} = \mathbf{B}'_{\eta_1((i,j))}^{(t)} \quad (69)$$

Before trying to prove (69), let's define κ_2, τ_2 and η_2 analogously:

$$\kappa_2(i) = \begin{cases} \text{MOD}_{2m}(2+m), & \text{if } i \in \{2, 2+m\} \\ i, & \text{otherwise} \end{cases}$$

$$\tau_2((i, j)) = (\kappa_2(i), \kappa_2(j))$$

$$\eta_2((i, j)) = \begin{cases} \tau_2((i, j)), & \text{if } (i, j) \in S \\ (i, j), & \text{otherwise} \end{cases}$$

Thus, by symmetry, (69) is equivalent to

$$\forall t, \mathbf{B}_{i,j}^{(t)} = \mathbf{B}'_{\eta_1((i,j))}^{(t)} = \mathbf{B}'_{\eta_2((i,j))}^{(t)} \quad (70)$$

Because of the recursive relation (26), we will show (70) by induction on t . For the base case, it can be verified that

$$\mathbf{B}_{i,j}^{(0)} = \mathbf{B}'_{\eta_1((i,j))}^{(0)} = \mathbf{B}'_{\eta_2((i,j))}^{(0)} \quad (71)$$

thanks to the construction of $G^{[1]}$ and $G^{[2]}$. Moreover, if we define another permutation $V \times V$, ζ_1 :

$$\zeta_1((i, j)) = \begin{cases} (\text{MOD}_{2m}(i+m), \text{MOD}_{2m}(j+m)), & \\ \quad \text{if } j \in \{1, 1+m\}, i \notin \{2, 2+m\} \\ \quad \text{or } i \in \{1, 1+m\}, j \notin \{2, 2+m\} \\ (i, j), & \text{otherwise} \end{cases} \quad (72)$$

then thanks to the symmetry between (i, j) and $(i+m, j+m)$, there is

$$\mathbf{B}_{i,j}^{(0)} = \mathbf{B}_{\zeta_1((i,j))}^{(0)}, \mathbf{B}'_{i,j}^{(0)} = \mathbf{B}'_{\zeta_1((i,j))}^{(0)}$$

Thus, for the induction to hold, and since σ applies entry-wise, it is sufficient to show that

Lemma 25. *If*

$$\mathbf{B}_{i,j} = \mathbf{B}_{\zeta_1((i,j))}, \mathbf{B}'_{i,j} = \mathbf{B}'_{\zeta_1((i,j))} \quad (73)$$

$$\mathbf{B}_{i,j} = \mathbf{B}'_{\eta_1((i,j))} = \mathbf{B}'_{\eta_2((i,j))}, \quad (74)$$

then

$$L(\mathbf{B})_{i,j} = L(\mathbf{B})_{\zeta_1((i,j))}, L(\mathbf{B}')_{i,j} = L(\mathbf{B}')_{\zeta_1((i,j))} \quad (75)$$

$$L(\mathbf{B})_{i,j} = L(\mathbf{B}')_{\eta_1((i,j))} = L(\mathbf{B}')_{\eta_2((i,j))}, \quad (76)$$

Proof of Lemma 25: Again, by symmetry between (i, j) and $(i + m, j + m)$, (75) can be easily shown.

For (76), because of the symmetry between η_1 and η_2 , we will only prove the first equality. By Maron et al. (2018), we can express the linear equivariant layer L by

$$L(\mathbf{B})_{i,j} = \sum_{(k,l)=(1,1)}^{(2m,2m)} T_{i,j,k,l} \mathbf{B}_{k,l} + Y_{i,j}$$

where crucially, $T_{i,j,k,l}$ depends only on the equivalence class of the 4-tuple (i, j, k, l) .

We consider eight different cases separately.

Case 1 $i, j \notin \{1, 2, 1 + m, 2 + m\}$

There is $\eta_1((i, j)) = (i, j)$, and $(i, j, k, l) \sim (i, j, \eta_1((k, l)))$, and thus $T_{i,j,k,l} = T_{i,j,\eta_1((k,l))}$. Therefore,

$$\begin{aligned} L(\mathbf{B}')_{\eta_1((i,j))} &= L(\mathbf{B}')_{i,j} \\ &= \sum_{(k,l)=(1,1)}^{(2m,2m)} T_{i,j,k,l} \mathbf{B}'_{k,l} + Y_{i,j} \\ &= \sum_{\eta_1((k,l))=(1,1)}^{(2m,2m)} T_{i,j,\eta_1((k,l))} \mathbf{B}'_{\eta_1((k,l))} + Y_{i,j} \\ &= \sum_{(k,l)=(1,1)}^{(2m,2m)} T_{i,j,\eta_1((k,l))} \mathbf{B}'_{\eta_1((k,l))} + Y_{i,j} \\ &= \sum_{(k,l)=(1,1)}^{(2m,2m)} T_{i,j,k,l} \mathbf{B}'_{\eta_1((k,l))} + Y_{i,j} \\ &= \sum_{(k,l)=(1,1)}^{(2m,2m)} T_{i,j,k,l} \mathbf{B}_{k,l} + Y_{i,j} \\ &= \mathbf{B}_{i,j} \end{aligned}$$

Case 2 $i \in \{1, 1 + m\}, j \notin \{1, 2, 1 + m, 2 + m\}$

There is $\eta_1((i, j)) = (i, j)$, and $(i, j, k, l) \sim (i, j, \eta_2((k, l)))$, because η_2 only involves permutation

between nodes 2 and $2 + m$, while i and $j \notin \{2, 2 + m\}$. Thus, $T_{i,j,k,l} = T_{i,j,\eta_2((k,l))}$. Therefore,

$$\begin{aligned}
L(\mathbf{B}')_{\eta_1((i,j))} &= L(\mathbf{B}')_{i,j} \\
&= \sum_{(k,l)=(1,1)}^{(2m,2m)} T_{i,j,k,l} \mathbf{B}'_{k,l} + Y_{i,j} \\
&= \sum_{\eta_2((k,l))=(1,1)}^{(2m,2m)} T_{i,j,\eta_2((k,l))} \mathbf{B}'_{\eta_2((k,l))} + Y_{i,j} \\
&= \sum_{(k,l)=(1,1)}^{(2m,2m)} T_{i,j,\eta_2((k,l))} \mathbf{B}'_{\eta_2((k,l))} + Y_{i,j} \\
&= \sum_{(k,l)=(1,1)}^{(2m,2m)} T_{i,j,k,l} \mathbf{B}'_{\eta_2((k,l))} + Y_{i,j} \\
&= \sum_{(k,l)=(1,1)}^{(2m,2m)} T_{i,j,k,l} \mathbf{B}_{k,l} + Y_{i,j} \\
&= \mathbf{B}_{i,j}
\end{aligned}$$

Case 3 $j \in \{1, 1 + m\}$, $i \notin \{1, 2, 1 + m, 2 + m\}$
Analogous to case 2.

Case 4 $i \in \{2, 2 + m\}$, $j \notin \{1, 2, 1 + m, 2 + m\}$
There is $\eta_1((i, j)) = (i, j)$, and $(i, j, k, l) \sim (i, j, \eta_1((k, l)))$, because η_1 only involves permutation between nodes 1 and $1 + m$, while i and $j \notin \{1, 1 + m\}$. Thus, $T_{i,j,k,l} = T_{i,j,\eta_1((k,l))}$. Therefore, we can apply the same proof as for case 2 here except for changing η_2 's to η_1 's.

Case 5 $j \in \{2, 2 + m\}$, $i \notin \{1, 2, 1 + m, 2 + m\}$
Analogous to case 4.

Case 6 $(i, j) \in S$
Define one other permutation on $V \times V$, ξ_1 , as $\xi_1((i, j)) =$

$$\begin{cases} (\text{MOD}_{2m}(i + m), j), & \text{if } \text{MOD}_m(j) = 1, \text{MOD}_m(i) \neq 1 \text{ or } 2 \\ (i, \text{MOD}_{2m}(j + m)), & \text{if } \text{MOD}_m(i) = 1, \text{MOD}_m(j) \neq 1 \text{ or } 2 \\ (i, j), & \text{otherwise} \end{cases}$$

It can be verified that

$$\xi_1 \circ \tau_1 = \eta_1 \circ \zeta_1$$

Moreover, it has the property that if $(i, j) \in S$, then

$$(i, j, k, l) \sim (i, j, \xi_1(k, l))$$

because ξ_1 only involves permutations among nodes not in $\{1, 2, 1 + m, 2 + m\}$ while $i, j \in \{1, 2, 1 + m, 2 + m\}$. Thus, we have

$$\begin{aligned}
(i, j, k, l) &\sim (\kappa_1(i), \kappa_1(j), \kappa_1(k), \kappa_1(l)) \\
&= (\tau_1(i, j), \tau_1(k, l)) \\
&= (\eta_1(i, j), \tau_1(k, l)) \\
&\sim (\eta_1(i, j), \xi_1 \circ \tau_1(k, l)) \\
&= (\eta_1(i, j), \eta_1 \circ \zeta_1(k, l)),
\end{aligned}$$

implying that $T_{i,j,k,l} = T_{\eta_1((i,j),\eta_1 \circ \zeta_1((k,l)))}$. In addition, as $\eta_1((i,j)) \sim (i,j)$, there is $Y_{\eta_1((i,j))} = Y_{i,j}$. Moreover, by (73),

$$\mathbf{B}'_{\eta_1 \circ \zeta_1((k,l))} = \mathbf{B}'_{\eta_1((k,l))} = \mathbf{B}_{k,l}$$

Therefore,

$$\begin{aligned} L(\mathbf{B}')_{\eta_1((i,j))} &= \sum_{(k,l)=(1,1)}^{(2m,2m)} T_{\eta_1((i,j),k,l)} \mathbf{B}'_{k,l} + Y_{\eta_1((i,j))} \\ &= \sum_{\eta_1 \circ \zeta_1((k,l))=(1,1)}^{(2m,2m)} T_{\eta_1((i,j),\eta_1 \circ \zeta_1((k,l)))} \mathbf{B}'_{\eta_1 \circ \zeta_1((k,l))} + Y_{\eta_1((i,j))} \\ &= \sum_{(k,l)=(1,1)}^{(2m,2m)} T_{\eta_1((i,j),\eta_1 \circ \zeta_1((k,l)))} \mathbf{B}'_{\eta_1 \circ \zeta_1((k,l))} + Y_{\eta_1((i,j))} \\ &= \sum_{(k,l)=(1,1)}^{(2m,2m)} T_{i,j,k,l} \mathbf{B}_{k,l} + Y_{i,j} \\ &= \mathbf{B}_{i,j} \end{aligned}$$

Case 7 $i, j \in \{1, 1+m\}$

There is $\eta_1(i, j) = (i, j)$ and $(i, j, k, l) \sim (i, j, \eta_2((k, l)))$. Thus, $T_{i,j,k,l} = T_{i,j,\eta_2((k,l))}$, and the rest of the proof proceeds as for case 2.

Case 8 $i, j \notin \{1, 1+m\}$

There is $\eta_1(i, j) = (i, j)$ and $(i, j, k, l) \sim (i, j, \eta_1((k, l)))$. Thus, $T_{i,j,k,l} = T_{i,j,\eta_1((k,l))}$, and the rest of the proof proceeds as for case 4.

□

With the lemma above, (69) can be shown by induction as a consequence. Thus,

$$\mathbf{B}_{i,j}^{(T)} = \mathbf{B}_{\eta_1(i,j)}^{(T)}$$

Maron et al. (2018) show that the space of linear invariant functions on $\mathbb{R}^{n \times n}$ is two-dimensional, and so for example, the second-last layer h in the 2-IGN can be written as

$$h(\mathbf{B}) = \alpha \sum_{i,j=(1,1)}^{(2m,2m)} \mathbf{B}_{i,j} + \beta \sum_{i=1}^{2m} \mathbf{B}_{i,i}$$

for some $\alpha, \beta \in \mathbb{R}$. Then since η_1 is a permutation on $V \times V$ and also is the identity map when restricted to $\{(i, i) : i \in V\}$, we have

$$\begin{aligned} h(\mathbf{B}'^{(T)}) &= \alpha \sum_{(i,j)=(1,1)}^{(2m,2m)} \mathbf{B}'_{i,j}^{(T)} + \beta \sum_{i=1}^{2m} \mathbf{B}'_{i,i}^{(T)} \\ &= \alpha \sum_{(i,j)=(1,1)}^{(2m,2m)} \mathbf{B}'_{\eta_1((i,j))}^{(T)} + \beta \sum_{i=1}^{2m} \mathbf{B}'_{\eta_1((i,i))}^{(T)} \\ &= \alpha \sum_{(i,j)=(1,1)}^{(2m,2m)} \mathbf{B}_{i,j}^{(T)} + \beta \sum_{i=1}^{2m} \mathbf{B}_{i,i}^{(T)} \\ &= h(\mathbf{B}^{(T)}) \end{aligned}$$

Therefore, finally,

$$m \circ h(\mathbf{B}^{(T)}) = m \circ h(\mathbf{B}'^{(T)})$$

□

K Deep Local Relational Pooling

Although we pre-compute $\pi \circ \mathbf{B}$ in the original version of Local Relational Pooling in Section 5 to make it feasible on synthetic data, it suffers from two drawbacks: 1) It only consists of a single LRP operation, therefore unable to exploit the non-local information beyond the depth- l egonet. 2) Its tensor representation and operations are fully dense, resulting in a quadratic cost for batched graphs, while a more reasonable cost would be linear with respect to batch size.

Hence, we propose a deep version of LRP with a typical layer illustrated in Figure 5 with operations defined as follows. Intuitively, instead of pre-computing $\pi \circ \mathbf{B}$, we pre-compute and store a mapping $\mathcal{I} : \mathbf{B} \mapsto C_k(\pi \circ \mathbf{B})$. Then, for static graphs, \mathcal{I} is iteratively used in each layer to perform an LRP operation. Note that this definition is mainly for a single graph $G = (V, E, x, e)$, but it is easy to generalize to a batch of graphs, which we will justify when necessary.

We use N to denote the total number of nodes in G , $|E|$ the total number of edges in G . We define P as the total number of permutations summed over all nodes in G . In other words, if we let P_i denote the number of size- k BFS permutations in the depth- l egonet of node i , then we have $P = \sum_{i=1}^N P_i$. We use $d^{(t)}$ to denote the hidden dimension on the t -th layer. Without loss of generality, we set $d^{(0)} = 1 + d_n + d_e$, where d_n, d_e are the dimensions of the given node and edge features, respectively, so that all information of the graph can be represented in a $n \times n \times d^{(0)}$ tensor, to be defined in (77). In deeper layers, the edge representation can be padded into $\mathbb{R}^{d^{(t)}}$ since typically $d_e \ll d^{(t)}$ for $t \geq 1$.

In Figure 5, we illustrate the operations in Deep LRP-1-4 where $l = 1$ and $k = 4$. In this example, the number 16 occurring in Figure 5 comes from the dimension of the flattening of a matrix in $\mathbb{R}^{4 \times 4}$, which would be replaced by k^2 when generalized to LRP of size k . Below, we comment on the operations involved in the model.

Tensor representation of an attributed graph: For an attributed graph $G = (V, E, x, e)$, we denote d_n as the dimension of node features, x_i 's, and d_e as the dimension of edge features, $e_{i,j}$'s. Then we define the third-order tensor representation of G as $\mathbf{B} \in \mathbb{R}^{n \times n \times (1+d_n+d_e)}$:

$$\begin{aligned} \mathbf{B}_{:, :, 0} &= A, \\ \mathbf{B}_{i, i, 1:d_n} &= x_i, \quad \forall i \in [n], \\ \mathbf{B}_{i, j, (d_n+1):(d_n+d_e)} &= e_{i,j}, \quad \forall (i, j) \in E, \end{aligned} \tag{77}$$

and any other entries not included in these formulas are set as 0.

Node_to_perm: This is a sparse matrix, denoted as $\mathbf{N2P}$, with size $(k^2 P \times N)$. The first dimension is from a flattened view of $k \times k$ entries for each permutation, where $k \times k$ is the size of the cropping. $\mathbf{N2P}$'s all nonzero entries are with a value of 1, and the corresponding position (i, j) stands for that the representation of node j appears in the i -th row for permutation representations. Hence,

$$\mathbf{N2P} : \mathbb{R}^{N \times \cdot} \rightarrow \mathbb{R}^{k^2 P \times \cdot},$$

where $\mathbb{R}^{N \times \cdot}$ is the space of node representations and $\mathbb{R}^{k^2 P \times \cdot}$ is the space of permutation representations.

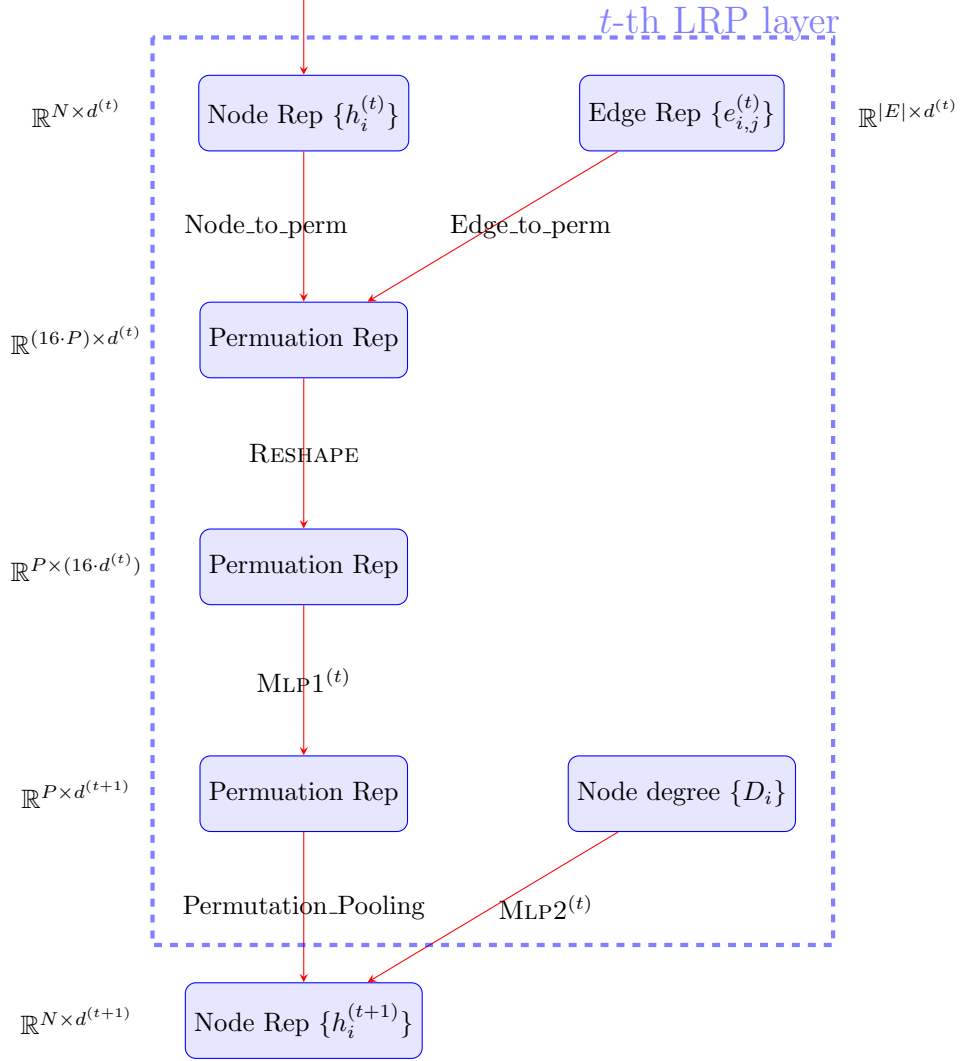


Figure 5: Illustration of the t -th local relational pooling layer in *Deep LRP-1-4*. Rounded rectangles denote representations (Rep) after each operation (denoted on arrows).

Edge_to_perm: This is a sparse matrix, denoted as $\mathbf{E2P}$, with size $(k^2P \times |E|)$. The first dimension is from a flattened view of $k \times k$ entries for each permutation, where $k \times k$ is the size of the cropping. $\mathbf{E2P}$'s all nonzero entries are with a value of 1, and the corresponding position (i, j) stands for that the representation of edge j (assume we have id for each edge) appears in the i -th row for permutation representations. Hence,

$$\mathbf{E2P} : \mathbb{R}^{|E| \times \cdot} \rightarrow \mathbb{R}^{k^2P \times \cdot},$$

where $\mathbb{R}^{|E| \times \cdot}$ is the space of edge representations and $\mathbb{R}^{k^2P \times \cdot}$ is the space of permutation representations.

Reshape: It is a tensor-reshaping operation that splits the first dimension from k^2P to $P \times k^2$.

MLP1: This is a trainable map from $\mathbb{R}^{\cdot \times (k^2d^{(t)})}$ to $\mathbb{R}^{\cdot \times d^{(t+1)}}$. We can utilize different activation functions in this component.

MLP2: This is a trainable map from \mathbb{R} to $\mathbb{R}^{d^{(t+1)}}$. We use ReLU as activation function. It is for learning a invariant function only dependent of node degree. The output dimension $d^{(t+1)}$ is typically larger than 1, with a goal of learning invariant function for various types of information.

Permutation_pooling: This is a sparse matrix, denoted as $\mathbf{Ppl} \in \mathbb{R}^{N \times P}$. Each of its non-zero entry (i, j) represents the contribution of the j -th permutation in the whole graph G to the representation of node i for the next layer. For example, sum-pooling corresponds to setting all non-zero entries in \mathbf{Ppl} as 1, while average-pooling corresponds to setting all non-zero entries in \mathbf{Ppl} as 1 and then normalizing it for every row, such as through the $\frac{1}{|S_{n_i,1}^{\text{BFS}}|}$ factor in (2).

Note that $\mathbf{N2P}$, $\mathbf{E2P}$ and \mathbf{Ppl} are compatible with batching several graphs. For instance, if there are m graphs to batch together and for $\alpha \in [m]$, $\mathbf{N2P}_\alpha \in \mathbb{R}^{k^2P_\alpha \times N_\alpha}$ is a sparse matrix for the α -th graph $G_\alpha = (V_\alpha, E_\alpha, \cdot, \cdot)$, then the $\mathbf{N2P}$ associated with the entire graph batch is of size $(k^2 \sum_{\alpha=1}^m P_\alpha) \times (\sum_{\alpha=1}^m N_\alpha)$, with $\mathbf{N2P}_\alpha$ being the diagonal blocks. This inserting operation is easy to implement since all these operations are stored as nonzero-index-value sparse matrices.

In summary, the update rule in the t th layer of a Deep LRP is given by:

$$h_i^{(t+1)} = \left[\mathbf{Ppl} \left[\text{MLP1}^{(t)} \left(\text{RESHAPE} \left(\mathbf{N2P}(\{h_i^{(t)}\}) + \mathbf{E2P}(\{e_{i,j}^{(t)}\}) \right) \right) \odot \text{MLP2}^{(t)}(\{D_i\}) \right] \right], \quad (78)$$

with $h_i^{(t+1)} \in \mathbb{R}^{N \times d^{(t+1)}}$. In the 0th layer, we set $h_i^{(0)} = x_i$.

Additionally, since we are interested graph-level tasks, the graph representation for a T -layer LRP is

$$f_{\text{LRP}}(G) = \text{MLP3} \left(\text{sum/average}_{i \in V} h_i^{(T)} \right)$$

We can also incorporate additional techniques in this framework, such as Batch Normalization (Ioffe and Szegedy, 2015), residual connection (He et al., 2015), and Jumping Knowledge (Xu et al., 2018b).

L Specific GNN architectures

In Section 6, we show experiments on synthetic and real datasets with several related architectures. Here are some explanation for them:

- **LRP- i - j** : Local Relational Pooling with egonet depth i and cropped subtensors of size j , as described in the main text. In our experiments, we take $i = 1, j = 4$. Hence, the vectorized subtensor (or submatrix, as the graph is unattributed) is of size $4 \times 4 = 16$. The nonlinear activation functions are chosen between ReLU and tanh by hand. The models are trained using the Adam optimizer [Kingma and Ba \(2014\)](#) with learning rate 0.1. The number of hidden dimensions is searched in $\{1, 8, 16, 64, 128\}$.
- **Deep LRP- i - j** : The Deep Local Relational Pooling with egonet depth i and cropped subtensors of size j , as described in Section 5. We take $i = 1, j = 4$. The nonlinear activation functions are ReLU. For synthetic experiments, we set the depth of the model as 1. The number of hidden dimensions is searched in $\{64, 128\}$. The final graph-level aggregation function is `sum`. For real experiments, we search the depth of the model in $\{4, 5, 6, 7, 8, 10\}$. The number of hidden dimensions is searched in $\{50, 100, 128, 150, 200, 256, 300, 512\}$. The final graph-level aggregation function is `average`. We involve Batch Normalization ([Ioffe and Szegedy, 2015](#)) and Jumping Knowledge ([Xu et al., 2018b](#)). On `ogbg-molhiv`, we utilize `AtomEncoder` and `BondEncoder` following the official implementation of GIN ([Xu et al., 2018a](#)) on the OGB leaderboard ([Hu et al., 2020](#)). The models are trained using the Adam optimizer [Kingma and Ba \(2014\)](#) with learning rate searched in $\{0.01, 0.005, 0.001, 0.0001\}$.
- **2-IGN**: 2nd-order Invariant Graph Networks proposed by [Maron et al. \(2018\)](#). In our synthetic experiments, we take 8 hidden dimensions for invariant layers and 16 hidden dimensions for output multi-layer perceptron. The models are trained using the Adam optimizer with learning rate 0.1. The numbers of hidden dimensions are searched in $\{(16, 32), (8, 16), (64, 64)\}$.
- **Powerful-IGN**: A Powerful IGN proposed by [Maron et al. \(2019b\)](#). In our synthetic experiments, we take the depth of the model as 4 and the hidden dimension in $\{16, 64\}$. The models are trained using the Adam optimizer [Kingma and Ba \(2014\)](#) with learning rate searched in $\{0.01, 0.001, 0.0001, 0.00001\}$. The depth of each involved MLP is 2.
- **GCN**: Graph Convolutional Networks proposed by [Kipf and Welling \(2016\)](#). In our experiments, we adopt a 4-layer GCN with 128 hidden dimensions. The models are trained using the Adam optimizer with learning rate 0.01. The number of hidden dimensions is searched in $\{8, 32, 128\}$. Depth is searched in $\{2, 3, 4, 5\}$.
- **GIN**: Graph Isomorphism Networks proposed by [Xu et al. \(2018a\)](#). In our experiments, we adopt a 4-layer GIN with 32 hidden dimensions. The models are trained using the Adam optimizer with learning rate 0.01. The number of hidden dimensions is searched in $\{8, 16, 32, 128\}$.
- **sGNN**: Spectral GNN with operators from family $\{\mathbf{I}, \mathbf{A}, \min(\mathbf{A}^2, 1)\}$. In our experiments, we adopt a 4-layer sGNN with 128 hidden dimensions. The models are trained using the Adam optimizer with learning rate 0.01. The number of hidden dimensions is searched in $\{8, 128\}$.

For GCN, GIN and sGNN, we train four variants for each architecture, depending on whether Jumping Knowledge (JK) ([Xu et al., 2018b](#)) and Instance Normalization (IN) / Spatial Batch Normalization ([Ulyanov et al., 2016](#); [Ioffe and Szegedy, 2015](#)) are included or not. The use of IN in GNNs is seen in [Chen et al. \(2019a\)](#), in which normalization is applied to each dimension of the hidden states of all nodes in each graph. For 2-IGNs, as IN is not immediately well-defined, we only train two variants, one with JK and one without. All models are trained for 100 epochs. Learning rates are searched in $\{1, 0.1, 0.05, 0.01\}$. We pick the best model with the lowest MSE loss on validation set to generate the results.

M Additional synthetic experiment results

On synthetic data, we design five substructure-counting tasks with patterns illustrated in Figure 3. In Section 6, we show results for 3-stars and triangles. In this section, we give results for the

remaining three patterns: tailed triangles, chordal cycles and attributed triangles. LRP-1-4, Deep LRP-1-4 and PPGN perform well for the induced-subgraph-count task of these three patterns on these two synthetic datasets, except that LRP-1-4 and PPGN have relatively large errors when counting attributed triangles on Random Regular data.

Table 4: Performance of different GNNs on learning the induced-subgraph-count of tailed triangles, chordal cycles and attributed triangles on the two datasets, measured by test MSE divided by variance of the ground truth counts (in Table 5). Shown here are the best and the median performances of each model over five runs. †: “dp” stands for a 1-layer model of the *Deep* implementation defined in Section K. *: after our search for hyperparameters, we report negative results that are not as good as those on Erdős-Renyi data.

	Erdős-Renyi				Random Regular			
	Tailed Triangle		Chordal Cycle		Tailed Triangle		Chordal Cycle	
	top 1	top 3	top 1	top 3	top 1	top 3	top 1	top 3
LRP-1-4	7.61E-5	1.94E-4	5.97E-4	7.73E-4	9.80E-5	2.01E-4	8.19E-5	1.63E-4
LRP-1-4 (dp)†	3.00E-6	1.25E-5	8.03E-6	9.65E-5	1.37E-7	2.25E-5	7.54E-13	3.22E-7
PPGN	7.11E-3	2.03E-2	2.14E-2	1.31E-1	2.29E-3	6.88E-3	5.90E-4	3.12E-2

	Erdős-Renyi		Random Regular	
	Attributed Triangle		Attributed Triangle	
	top 1	top 3	top 1	top 3
LRP-1-4	9.23E-4	2.12E-3	4.50E-1*	4.72E-1*
LRP-1-4 (dp)†	1.48E-4	1.35E-3	9.06E-5	5.05E-4
PPGN	2.58E-5	8.02E-5	4.30E-1*	4.33E-1*

Table 5: Variance of the ground truth labels for all synthetic tasks.

Task	Erdős-Renyi	Random Regular
3-star	311.20	311.20
triangle	7.3441	9.4249
tailed triangle	607.78	1472.93
chordal cycle	86.48	102.58
attributed triangle	2.11	2.71

N Experiments on molecule datasets

Datasets. We adopt molecule datasets *ogbg-molhiv* (Wu et al., 2018; Hu et al., 2020) and *QM9* (Ramakrishnan et al., 2014; Wu et al., 2018) for real experiments. *ogbg-molhiv* is with 41127 graphs, 25.5 nodes per graph, 27.5 edges per graph and 1 target task. Each graph represents a molecule, where nodes are atoms, and edges are chemical bonds. OGB Hu et al. (2020) adopts the *scaffold splitting* procedure that splits the molecules based on their two-dimensional structural frameworks. The scaffold splitting attempts to separate structurally different molecules into different subsets, which provides a more realistic estimate of model performance in prospective experimental setting (Wu et al., 2018). *QM9* is with 134K graphs and 12 target tasks. The data is randomly split into 80% train, 10% validation and 10% test. On both datasets, we report the test error corresponding to the epoch with best validation performance.

Loss and Evaluation. For *ogbg-molhiv*, we set the loss function as Binary Cross Entropy. we utilize the official APIs including an evaluator provided by OGB (version 1.1.1) (Hu et al., 2020). For *QM9*, we set the loss function as the 12-class average of normalized Absolute Errors where normalization stands for an absolute error divided by the standard deviation of labels in the corresponding class.

We report such average normalized errors as “Loss” in Table 3. The un-normalized 12-class Mean Absolute Errors are also reported.

Training Epochs. In `ogbg-molhiv`, scaffold splitting (Wu et al., 2018) separates structurally different molecules into different subsets, so more training epochs might bring worse generalization performance. Hence, we report two results of LRP-1-4 on `ogbg-molhiv` in Table 2 where “LRP-1-4” is trained for 100 epochs while “LRP-1-4 (ES)” is another model with a different group of hyperparameters trained for only 20 epochs. To ensure the reproducibility of our results, LRP-1-4 (ES) is run with 35 random seeds, from 0 to 34. Note that baselines on the OGB leaderboard are reported to be trained for 100 epochs with 10 runs.

Running Time. We report the average training time of Deep LRP-1-4 on `ogbg-molhiv` in Table 6. Our implementation is based on Deep Graph Library (DGL) (Wang et al., 2019) and the GIN implementation is transferred from its official implementation for `ogbg-molhiv` on PyTorch Geometric (Fey and Lenssen, 2019) to DGL. We can see that Deep LRP-1-4 approximately takes $\sim 4\times$ time as much as GIN. However, the proportion goes down to 1.2-2 \times when we utilize more numbers of workers to load the data, because the dataloader involves batching operations as defined in Appendix K. Also note that Ours-2 and Ours-3 are slower than Ours 1 since both of them use Batch Normalization while the latter does not, and Batch Normalization turns out to slow down the models in our experiments.

Table 6: Training time per epoch for different GNNs on `ogbg-molhiv` with batch size of 64. All results are generated from a computing node with a GTX 1080Ti, 8 CPUs and 64GB RAM. “#workers” stands for the number of workers in Dataloader of PyTorch. “Ours-2” is the model reported as “LRP-1-4” in Table 2 while “Ours-3” is the model reported as “LRP-1-4 (ES)”.

model	time/epoch (sec)	#params	#workers
GIN	31	1.89M	0
GIN	29	1.89M	4
GIN	29	1.89M	8
Ours-1	132	2.07M	0
Ours-1	36	1.66M	4
Ours-1	36	1.66M	8
Ours-2	122	0.98M	0
Ours-2	57	0.98M	4
Ours-2	50	0.98M	8
Ours-3	134	6.30M	0
Ours-3	55	6.30M	4
Ours-3	58	6.30M	8